Calibration of TOPEX/Poseidon at Platform Harvest

E.J. Christensen, B.J. Haines, S.J. Keihm, C.S. Morris, R.A. Norman, G.H. Purcell, B.G. Williams, B.C. Wilson

Jet Propulsion Laboratory, California Institute of Technology

G.H. Born, M.E. Parke

Colorado Center for Astrodynamics Research, University of Colorado, Boulder

S.K. Gill

NOAA/National Ocean Service

C.K. Shum, B.D. Tapley

Center for Space Research, University of Texas, Austin

R. Kolenkiewicz, R.S. Nerem

NASA/Goddard Space Flight Center, Space Geodesy Branch

Submitted to the Journal of Geophysical Research
Special TOPEX/Poseidon Issue
December 1993

Calibration of TOPEX/Poseidon at Platform Harvest

E.J. Christensen, B.J. Haines, S.J. Keihm, C.S. Morris, R.A. Norman, G.H. Purcell, B.G. Williams, B.C. Wilson

Jet Propulsion Laboratory, California Institute of Technology

G.H. Born, M.E. Parke

Colorado Center for Astrodynamics Research, University of Colorado, Boulder

S.K. Gill

NOAA/National Owan Service

C.K. Shum, B.D. Tapley

Center for Space Research, University of Texas, Austin

R. Kolenkiewicz, R.S. Nerem

NASA/Goddard Space Flight Center, Space Geodesy Branch

Abstract: We present preliminary estimates for the mean bias of the TOPEX/Poseidon NASA altimeter (ALT) and the CNES altimeter (SSALT) using in situ data gathered at platform Harvest during the first 36 cycles of the mission. Data for 21 overflights of the ALT and 3 overflights of the SSALT have been analyzed. The analysis includes an independent assessment of in situ measurements of sea level, the radial component of the orbit, wet tropospheric path delay, and ionospheric path delay. Tide gauges at Harvest provide estimates of sea level with an uncertainty of&2. 1 cm. The uncertainty in the radial component of the orbit is estimated to be ±1.6 cm. In situ measurements of tropospheric path delay at Harvest compare to within ±1.3 cm of the TMR, and in situ measurements of the ionospheric path delay compare to within -0.4 ±0.7 cm of the dual-frequency ALT and 1.1 ±0.6 cm of DORIS. We obtain a bias estimate of -14.7 ±2.1 cm for the ALT and +2.9 ±2.4 cm for the SSALT, which are consistent with independent estimates for the relative bias between the two altimeters, (The sign convention is such that a correction to absolute sea level derived from the GDR altimeter data can be obtained by algebraically adding the bias to the data.)

A linear regression applied to the complete set of data indicates a secular trend in the ALT bias of 3.6 ±2.4 cm/yr. If data for the first 15 cycles is excluded from the analysis, the estimated slope is negligible. A candidate explanation is that this 'drift' is introduced by an error in the in situ measurements of sea level that is proportional to sea state. A portion of this error may also be due to EM-bias. An extension of the time series for the bias estimates is needed to better understand this trend, particularly into the '93-'94 winter season where the sea state is expected to be high.

1. INTRODUCTION

TOPEX/Poseidon employs two fundamental measurements to arrive at observations of sea level, radar altimetry and orbit determination. The radar altimeter observes the height of the satellite above the ocean surface and orbit determination observes the distance of the satellite relative to the center of Earth, usually expressed as the height of the satellite above the reference ellipsoid. The difference between these two measurements is sea level relative to the reference ellipsoid. Given corresponding in situ measurements of sea level, an independent check on altimetric observations can be made. This procedure, referred to as closure, is basically the approach

followed at three verification sites; the Harvest platform off the coast of California near Point Conception, Lampedusa Island in the Mediterranean Sea, and the Bass Strait near Burnie, Australia [Christensen and Menard, 1992].

This paper will focus on the closure results obtained at the highly instrumented oil platform at Point Conception, established by NASA to gather in situ data necessary to *verify* the performance of the NASA altimeter (ALT) and the CNES altimeter (SSALT). (For results obtained from the CNES verification site at Lampedusa, see Menard et at. [this issue], and from the Australian site at Burnie, see White et al. [this issue].) A comparison of altimetric and in situ data obtained for each overflight leads to bias estimates for each of the two altimeters, i.e. the difference between the altimeter-t-ocean distance observed by the altimeter and that derived from orbit and in situ sea level measurements. (It is important to point out that referring to mis-closure as altimeter bias is a misnomer. A bias can originate in the tropospheric path delay calibration, ionospheric path delay calibration, the orbit, or the in situ systems themselves. Keeping with tradition, and for the sake of brevity, we will refer to the mis-closure as 'altimeter bias".) Knowledge of the altimeter bias lends itself to the analysis of sea level data obtained from more than one altimetric system, e.g. SeaSat, GeoSat, and TOPEX/Poseidon itself. If the bias estimate is sufficiently accurate, long-term trends in sea level can be obtained from extant and future altimeter missions. More importantly, any significant drift in the bias of an altimetric system can be mistaken for a temporal variation in the sea surface.

The altimeter calibration technique employed for the current analysis is similar to that used for the assessment of the SeaSat bias by Kolenkiewicz and *Martin* [1982] *at* Bermuda, and the ERS-1 bias by Wakker, et al. [1991] and Scharroo et at. [1991] at the Venice Tower. The methodology is illustrated in Figure 1.1 where, as the satellite overflies the platform, it is observed by the Satellite Laser Ranging (SLR), Global Position System (GPS), and Doppler Orbitography and Radio-positioning Integrated by Satellite (DORIS) tracking systems. The altitude of the satellite relative to the reference ellipsoid at the time-of-closest-approach (tea) to the platform is determined *using* both long-arc (-1 -day and 10-day) and short-arc (~1 5-rein) orbit determination techniques, The position of the verification site relative to the reference ellipsoid is established by reducing data obtained from a GPS receiver located at the site. In situ measurements of sea level relative to the GPS receiver are obtained from tide gauges installed at the platform. A detailed description of each these fundamental measurements and a preliminary assessment of the data obtained during the first twelve months of TOPEX/Poseidon operations are presented in this paper.

2. VERIFICATION SITE

The two most critical criteria for selection of the NASA verification site were the extent of laser coverage and the anticipated accuracy of in situ measurements. Practical issues, such as logistics and cost, were also discriminating factors. Consideration was given to the island of Bermuda, oil platforms in the Gulf of Mexico, and

oil platforms off the coast of California. Based on excellent laser coverage (see section 5) and logistics, Texaco's Platform Harvest, located at 34.470923°N latitude and 239.314155°E longitude, was chosen, It is situated 19 km west of Point Conception, California and 11.5 km off the coast of California as measured along the TOPEX/Poseidon groundtrack corresponding to ascending pass number 43 (see Figure 2.1). In March 1991, a Memorandum of Understanding was signed between Texaco USA, Inc. and the Jet Propulsion Laboratory (JPL) permitting the installation of in situ instruments at Harvest. For a more complete description of the instrumentation at the platform, see Morris et at. [1994].

2.7 *Tide Gauges*

The expected accuracy of sea level measurements at the platform was difficult to estimate since experience with precision tide gauges in near open-ocean has been very limited, particularly in the vicinity of such a large structure. Bottom" pressure gauges, which have been used extensively to measure tides in open-ocean [Filloux, 1980], were considered as an alternative to the platform; however, these instruments are notorious for bias drift due to creep and thereby do not satisfy our long-term accuracy requirements. In an attempt to ensure that in situ measurements of sea level would not compromise the closure results, three tide gauges were installed at different locations around the platform.

A team of scientists and engineers from the Jet Propulsion Laboratory (JPL), the NOM/National Ocean Service (NOS), and the University of Colorado, Boulder (CU) was responsible for all aspects of the design, installation, and maintenance of the in situ instruments. They were faced with the formidable challenge of meeting exacting accuracy requirements in a relatively harsh ocean environment. Restrictions and limitations associated with working on an oil platform made the task even more challenging. Table 2.1 provides a summary of the instruments and Figure 2.2 illustrates their relative location on the platform.

NOAA/NOS provided two of the three tide gauges installed at the platform, an acoustical device and a nitrogen-bubble, which comprise the Next Generation Water Leveling Measuring System (NGWLMS) [Gill et at., 1994]. The NGWLMS is a setf calibrating device that uses the time delay of an acoustical pulse reflected from the ocean surface to measure sea level. The bubbler derives sea level from the change in the pressure of nitrogen gas as it flows through a submerged, open-ended tube. The University of Colorado (CU) provided the third tide gauge system which is comprised of three pressure transducers [Kubitschek et al., 1994]. Two of the pressure transducers are mounted at depth to measure hydrostatic pressure and the third above the water to measure atmospheric pressure. The pressure differential between the submerged and surface transducers vanes with sea level. The two submerged transducers provide redundancy and also can be used for internal calibration purposes. The third pressure transducer also serves as a backup to the NOAA/NOS barometer for measuring atmospheric pressure,

The data collection rates varied by system, Both NOAA/NOS systems collected low-rate data on six minute

centers most of the time. For a majority of the overflights, the NGWLMS collected high-rate data using the 'Tsunami Modem, which produces a sample every two seconds. The CU system collected low-rate data on 82,4 second centers, with 1.1 second high-rate sampling during most of the overflights.

2.2 TurboRogue Receivers

To obtain accurate estimates for the vertical component of the platform's position relative to the reference ellipsoid, two TurboRogue GPS receivers, one placed at Harvest and the other at a SLR site near Quincy, California, were used to perform a geodetic survey of the two sites. Knowledge of the baseline between Harvest and Quincy permits us to tie orbits determined with SLR, DORIS, and GPS data into the same reference frame. This ensures that no mis-closure will result from potential inconsistencies in the coordinate systems used to generate ephemerides based on different tracking systems. *A* more detailed discussion of the subject can be found in Section 4.

The TurboRogue GPS receiver installed at Harvest also provides an estimate for the total electron content (TEC) of the ionosphere along the electromagnetic path of the altimeter for each overflight. To corroborate our closure results, the derived TEC is converted to path delay at Ku-band which serves as a check on values obtained from the dust-frequency ALT and DORIS. A more detailed discussion of this topic can be found in Section 7.

2.3 *Water Vapor Radiometer*

During the site-selection process, a number of issues associated with the relative proximity of Harvest to land had to be taken into consideration. At Point Conception, land is out of range of the altimeter until approximately one second after tea. Even though a longer span of data distributed symmetrically about the platform would be preferred, this is not considered to be a serious drawback. However, due to its significantly larger footprint, the TOPEX/Poseidon Microwave Radiometer (TMR) observations of wet tropospheric path delay are almost certainty contaminated by land at Harvest. In anticipation of this problem, a JPL J-Series WVR was installed at the platform to provide an alternative means for obtaining the wet tropospheric path delay correction for the altimeters (see Section 6).

2.4 *Ancillary Equipment*

Ancillary measurements of relative humidity, barometric pressure, water temperature, water conductivity, and air temperature are made by NOAA/NOS instruments. Some of these measurements, such as barometric pressure, water temperature and conductivity, are crucial to the proper reduction of the pressure transducer data used for obtaining measurements of sea level.

The computers associated with the verification instrumentation at the platform are housed in a small custom-made equipment shed. In addition to collecting and storing data, equipment in the *shed* provide clean power and communications via the GOES satellite (NOAA/NOS data only) and cellular telephone.

3. PRE-LAUNCH ERROR BUDGET

Table 3.1 is the error budget for the in situ system at the platform for a single overflight of the ALT. The errors are characterized as either fixed or variable, in a temporal sense. The fixed error pertains to the absolute knowledge and the variable error pertains to the random nature of the altimeter bias estimates from pass-to-pass. For example, the location of the oil platform relative to the laser sites is dependent on the accuracy of the GPS survey. Prior to launch, it was estimated that the baseline could have a fixed error as large as 2.0 cm; however, there is afso a random component that enters the daily estimates of the vertical because of data noise, atmospheric delays, multi-path, and changing geometry of the GPS constellation. It is important to note that fixed errors are not observable, i.e. a fixed error will be absorbed directly into the altimeter bias estimate. Further, an increasing number of "independent estimates will result in a corresponding reduction of the variable error whereas a fixed error can onty be reduced through more accurate calibration of the measurement systems..

There are a number of errors associated with in situ measurements of sea level. The largest of these is the variable error that is expected to result from the variability of the ocean within the altimeter footprint. That is, the mean temporal sea level obtained from a tide gauge may not be exactly comparable to the mean spatial sea level observed by the altimeter. Therefore, based mostly on our nescience, we assume a variable error of $\pm$2.0 due to the uncertainties in the effects of ocean variability on the aftimeter and tide gauge measurements.

Prior to launch, our ability to observe sea level with the requisite precision using tide gauges in open-ocean was uncertain, yet we expected that the performance of a three-tide-gauge system would be comparable to that obtained with a coastaf tide gauge. Since launch, analysis of in situ sea level data gathered at Harvest reveal significant inconsistencies among the three tide gauges. Differences as large as 2.0 -4.0 cm were observed to persist for periods ranging from hours to weeks. As discussed by Parke and Gill [1992], at least some of these inconsistencies are now understood. However, the 1.0 cm variable error assumed for in situ measurements of sea level may prove to be optimistic.

An error in our knowledge of the cross-track gradient for the geoid can introduce a measurable error in closure as the groundtrack of the satellite varies within $\pm$1.0 kilometer of the platform in the cross-track direction, Even though our a priori knowledge of the geoid gradient at Harvest is thought to be relatively good, it is anticipated that it can be improved by estimating a correction term that is proportional to the distance-at-closest-approach (dca), provided the gradient is adequately sampled over time.

The expected error for the ensemble in situ measurements is $\pm$2.06 cm for the variable part, $\pm$2.60 cm for

the fixed part, for a total of ±3.5 cm for a single overflight. When the expected errors in the altimeter measurement [Born et al., 1984] and orbit (see Section 5) are included (Table 3.2), it is anticipated that the absolute altimeter bias can be determined to within ±3.9 cm for the variable part, ±3.4 cm for the fixed part, for a total of ±5.2 cm for a single overflight (see Table 3.3). The variable component of this error will result in a decrease in the uncertainty of the mean bias estimate as the number of overflights increase (see Table 3.3); however, the fixed error represents a noise-floor beyond which we cannot expect any improvement using the current data set. (Note that the variance on the mean is derived from linear regression, therefore the variable portion of the single-pass variance decreases by $4n^{-1}$, not n^{-1}.) The results presented in this paper suggest that the performance projected by the pre-launch error budget is conservative.

4. GPS SURVEY

Observations obtained with GPS receivers provide an estimate for the vector separation between a monument (geodetic marker) mounted on platform Harvest, and a monument collocated with the SLR tracking station near Quincy, California, This measurement can then be combined with the relative offset between the GPS and SLR monuments at Quincy, and the relative offset between the GPS and tide gauge monuments at Harvest, to obtain the location of the ocean surface in the appropriate reference frame. Alternatively, the geocentric height of the Harvest platform, i.e. the height relative to the reference ellipsoid, can be estimated directly. The dual-frequency GPS measurements at Harvest also provide estimates for the total electron content (TEC) of the ionosphere at zenith which are later used to calibrate the dual-frequency altimeter and DORIS (see Section 7).

4.1 *Data Collection and Analysis*

With a few exceptions, GPS data were collected on a fairly continuous basis at both Quincy and Harvest throughout the verification period. These data were divided into day-long segments, yielding an independent daily estimate of the Quincy-Harvest baseline. These daily estimates are capable of reveating variation on the order of a centimeter per year in the coordinates for Harvest and Quincy that may result *from* tectonic plate motion or subsidence of the oil platform. High frequency variations arising from unmodeled effects, such as ocean loading, are also detectable, (Note that errors due to diurnal variations in ocean loading average to nearly zero for the daily fits.) The analysis described in this section was performed at the Jet Propulsion Laboratory using the Global Inferred Position System (GIPSY) analysis software. For more details on the processing of the data, see Purcell et al. [1994]

Apart from occasional outages, daily estimates for the baseline between Quincy and platform Harvest have been obtained between September 25, 1992 and October 1, 1993. Atthough this interval extends well beyond the

end of the formal verification period, the additional data contribute significantly to the final estimate of the baseline, particularly the linear rate of change of the baseline, We were not able to obtain solutions for certain days for a variety of reasons. One of the receivers would occasionally malfunction so that, at times, there were not enough data to yield meaningful results. The most significant outage began on Christmas day 1992 and continued into early January 1993. Data loss also occurred during periods when the signals from some of the GPS satellites were encrypted. Although the receivers continued to operate, the software was unable to cope with the peculiarities 01 the data. (This problem was most acute at times when some receivers in the global network were observing a satellite in the normal ● P-codem mode, while others were observing it in the 'cross-correlation' mode for encrypted data.) As verification proceeded, episodes of encryption involved more satellites and lasted longer. For example, the days April 19-24, April 28-May 3, and June 5-9, l993 were conspicuously affected by encrypted data and are not included in the final results. The most significant loss of data occurred when a blanket of snow covered the antenna at Quincy from January 5 until February 19, l993. Even after the snow melted, the station did not return to normal operation until the GPS receiver was replaced on March 25, 1993. As a result, 80 days of the data at Quincy were lost. Despite the missing data, we have more than an adequate number of observations for determining the Quincy-Harvest baseline with the requisite accuracy of 2 cm in the vertical.

Up until the time of the large data gap, the procedure for reducing GPS paralleled that used for the daily global Fiducial Laboratory for an Integrated National science Network (FUNN) analysis; thereafter, the solutions were obtained directly from the FUNN analysis. On December 8; 1992, the original strategy was modified slightly in two ways: first, an improved gravity model (JGM-2) was introduced "into the GPS orbit analysis; and second, the fiducial stations locations were not held fried, rather they were updated on a daily basis using the International Terrestrial Reference Frame plate motion model adopted in l991(ITRF91) [Boucher and Altamimi, l991]. A comparison of the December 8, l992 baseline estimates obtained with the new and the oid models showed that the effects of these changes are negligible.

4.2 Baseline Estimates

The solutions for the vertical component of the baseline between Quincy and Harvest are shown in Figure 4.1. The error bars represent the formal uncertainties ascribed to the estimates by the GIPSY analysis software. Weighted linear fits to the time series, represented by the dotted lines, indicate the secular drift rate and the scatter of the data. The formal uncertainties for these estimates are less than 1 mm and the uncertainties for their rates are less than 3 mm/year. However, in practice, unmodelled effects introduce errors that are somewhat larger than the formal uncertainties. Based on the FUNN analysis, the secular trend of -1.3 cm/yr may be attributable to plate motion at Quincy, in which case the subsidence at the platform during the interval studied would be negligible.

Figure 4.2 shows the height of Harvest relative to the reference ellipsoid obtained by solving for tha geocentric coordinates for the platform directly. Note that this analysis corroborates our observation that Harvest

is not subsiding during this time period. Also note that solutions were obtained for the 80 days that the Quincy antenna was under snow. The direct estimate for the vertical height, as defined in ITRF91, is 15.67 m, which is the number used for our closure analysis. The height estimate obtained using the baseline vector estimate, combined with the station location for Quincy expressed in the SSC93L07 coordinate system, is 15.69. The SSC93L07 coordinate system, which is close to ITRF92 [Boucher and Altamimi, 1992], has been adopted by GSFC and CSR for POE production, (see Tapley et al. [this issue]). At least part of the 2 cm discrepancy in the height estimates is due to differences in the ITRF91 and SSC93L07 coordinate systems.

5. ORBIT DETERMINATION

The altimeter range supplies only hatf of the information necessary to determine sea level. The other critical measurement is the radial height of the spacecraft above the reference ellipsoid of the Earth which is obtained from satellite tracking date through the process of orbit determination. Any error in the radial height measurement will map directly into altimeter bias estimates. Errors in the force models used to integrate the satellite trajectory, as well as the noise and distribution of the tracking data, wiii impact the accuracy of the computed radial height of the spacecraft.

The pm-launch error budget for TOPEX/Poseidon projected that the global root-mean-squared (rms) error in the orbital height of TOPEX/Poseidon would be on the order of 13 cm [Born et al., 1984]. Due to the substantial efforts of the precision orbit determination (POD) team during the development phase of mission, the height can actually be computed with global rrns accuracies of 3-5 cm using the SLR, DORIS, and GPSDR tracking systems [Tapley et al., this issue and Bertiger et al., this issue], As discussed below, orbit knowledge at platform Harvest is remarkably better than this, partly due to the accuracy of the gravity model and large number of SLR and DORIS , tracking stations in the eastern Pacific Ocean, and the nearly continuous coverage afforded by GPS.

5.1 *SLR ● nd DORIS Long-Arc Orblts*

A network of 10 to 15 satellite laser ranging (SLR) stations [see Tapley, et al. this issue] is the NASA baseline tracking system for precision orbit determination (POD) and the calibration of the two radar altimeters at Harvest. The DORIS tracking system is the CNES baseline tracking system which uses microwave Doppler techniques for POD. The system is composed of an on board receiver and a network of 40 to 50 ground transmitting stations [see Nouel, et al. this issue], providing ail-weather, global tracking of the satellite. The signals are transmitted at two frequencies (401.25 MHz and 2036.25 MHz) to allow removal of the effects of ionospheric free electrons in the tracking data. Therefore, the total content of the ionospheric free electrons can also be estimated from the DORIS data and used for the ionospheric correction for the SSALT.

Since the tracking provided by SLR and DORIS is not continuous in time, orbit determination based on dynamical equations is required to produce precise orbits for the mission. Prior to launch, the knowledge of Earth's gravity field was considered to be the limiting error source for POD, so both NASA and CNES established special teams to develop a much improved Earth gravity model. As described by Nerem, et al. [this issue] and Tapley, et al. [this issue], this effort led to a pre-launch model (JGM-1) that was expected to perform even better than 13,0 cm rms. JGM-1 achieved 3.4 cm rms and the TOPEX/Poseidon tuned gravity model (JGM-2) improved the performance even further to 2.2 cm rms [Christensen et al., 1994]. As discussed later in this section, orbit errors introduced by the JGM-2 gravity model over Harvest are remarkably small (-1.0 cm). As a result, non-gravitational forces due to drag and solar radiation, and the definition of the terrestrial reference frame (station locations) are now considered to be the limiting error sources for POD.

Precision orbit ephemerides (POEs) provided by Goddard Space Flight Center (GSFC) for routine Geophysical Data Record (GDR production were included in the dosure analysis. These orbits were determined from SLR and DORIS data gathered over 10-day arcs corresponding to each cycle of the mission. The dynamic models include the JGM-2 gravity field and a quasi-empirical box-wing model for the non-gravitational forces. The data are processed in a batch-mode where the spacecraft state at epoch and daily parameters representing constant and once-per-revolution acceleration parameters in the along-track and orbit-normal directions are estimated. A complete description of the POES is given by Nerem et al. [this issue] and Tapley et al. [this Issue].

The Center for Space Research (CSR) atso produced precision orbit ephemerides that were included in the dosure analysis. These orbits are determined from SIR and DORIS data gathered over 1-day arcs centered about the time of the Harvest overflights. The dynamic models indude the TEG-3 gravity model, which is JGM-2 tuned with GPS flight data from TOPEX/Poseidon, [Tapley et al., 1993] and empirical non-gravitational forces models. The data are processed in a batch-mode where the spacecraft state at epoch and daily parameters representing constant and once-per-revolution acceleration parameters in the along-track and orbit-normal directions are estimated. For a more complete discussion on CSR-Tuned orbits, see Tapley et al. [1993].

52 *SLR Short-Arc Orbits*

Short-arc orbit (SAO) determination is a technique used to obtain the best estimate for the radial component of an orbit by fitting satellite laser ranging (SLR) data obtained from two or more stations that track the satellite simultaneously. This corresponds to a time period less than 15 minutes for TOPEX/Poseidon. During an overflight of platform Harvest, the satellite can be observed by as many as four SLR stations at the same time: Quincy, CA; Monument Peak, CA Mazatlan, Mexico; and McDonald Observatory at Ft. Davis, TX. A representation of the coverage along the groundtrack for pass number 43 is shown in Figure 5.1. Note that the circles indicated in the figure are defined by a 15° minimum elevation limit, Note that it is *not* likely that laser tracking data will be obtained by all stations for every overflight since SLR stations operate at optical wavelengths which are obscured

during cloudy or foggy weather.

The TOPEX/Poseidon SAO determination capability at JPL has been developed in parallel with the precision orbit determination system (PODS) processing capability at Goddard Space Flight Center at Greenbelt, Maryland, the University of Texas Center for Space Research at Austin, Texas and the Colorado Center for Astrodynamics Research at Boulder, Colorado. The JPL. development team has been aided by, and has participated in, the development of specific POD models for TOPEX/Poseidon. Since SAO accuracy is most sensitive to the accuracy of geometric models used in the orbit determination procedure, particular attention was given to modeling the ground station coordinates, solid Earth tides, tropospheric range correction, Earth rotation and polar motion parameters, spacecraft center of mass offset from the laser retro-reflector assembly (LRA), and spacecraft orientation. The box-wing model mentioned above was used to model the orientation of the LRA relative to the spacecraft center-of-gravity; however, for reasons that will be explained below, the forces predicted by the box-wing model were not used to produce SAOs.

A covariance analysis was performed for the calibration overflights at Harvest to determine the best tracking geometry and the limiting error sources for short arc orbit determination. The results shown that SAO technique produces precise estimates for the orbit position relative to a local tracking network [Williams et al., 1993]. Both the covariance analysis and post-launch results show that SAO accuracy depends primarily on favorable tracking geometry and is relatively insensitive to mis-modeled spacecraft dynamics. For the Harvest overflights, a minimum of two tracking stations located on each side of the ground track provided the best determination of orbit height. In addition, the analysis indicates that station location error is the limiting error source for determining orbit height at Harvest with the SAO technique.

Post-launch studies showed that the Keplerian orientation angles for the SAOs; inclination (INC), ascending node (OMEGA) and argument of periapsis (AOF'), are poorly determined if each of the six components of the spacecraft state are allowed to have full degree of freedom. This is detrimental to closure since orbit orientation errors map into altitude errors through the geoid gradient and orbital eccentricity. The fundamental strength of the SAO technique is its ability to observe the in-plane Keplerian coordinates of the orbit; semi-major axis (SMA), eccentricity (ECC) and time-from-periapsis (TFP), with extreme accuracy. Therefore, following Bonnefond et al. [this issue], a hybrid approach was used where the short-arc laser fit for each overflight was constrained to nominal values for the orbit orientation as prescribed by the appropriate long-arc precision orbit ephemeris (the NASA POE). For the SAO solutions, this constraint was obtained by transforming an a priori diagonal invariance matrix for the Keplerian orbit elements into an a priori covariance matrix for the Cartesian state vector at each epoch. The covariance matrix was constructed using the geometric relationship between Keplerian orbital elements and the radial, cross-track and down-track components of the orbit. Standard deviations of 1 m radial, 50 cm cross-track, and 15 m down-track were assumed, The allocation of these constraints to the Keplerian elements is given in Table 5.1.

5.3 *GPS Orbits*

The same basic principles used for geodetic positioning of GPS receivers are applied for the positioning of TOPEX/Poseidon. Multidirectional pseudorange and carrier phase data are collected simultaneously at ground stations and the spacecraft which are then combined over suitable periods of time --- typically a few hours to several days --- in order to determine the ephemerides of the orbiter [Yunck et al., 1994]. The simultaneous measurements from the ground stations can be combined to nearly eliminate the effects of dock errors and selective availability (SA) degradation, while also mitigating the effects of errors in the GPS ephemerides. The longer observing times are beneficial because consecutive carrier phase measurements can be smoothed to provide position change information. Additional benefit is derived from the pseudorange measurements, since they provide a powerful constraint on the ambiguity of the carrier phase differences. The overall approach is called 'differential GPS".

What makes the GPS approach especially attractive is that the robust observation geometry permits orbit solutions with minimal dynamic force model constraints on the spacecraft motion [Yunck and Wu, 1966], Errors in force models, especially the Earth gravity, are the principal limitation in traditional approaches to satellite orbit determination. However, force models can still be exploited to improve the accuracy of orbits obtained with GPS using what is referred to as the 'reduced dynamic technique [Wu et at., 1991 and Yunck et al,, 1994]. With this hybrid approach, unmodeled spacecraft accelerations are represented as a stochastic process, the characteristics of which are specified a priori to reflect the desired weighting of the dynamics and the geometry. When the geometry is strong, the unmodeled accelerations are readily observable; when the observability is weak, the force model constraints will prevent estimates for the orbit parameters from diverging, This is the fundamental approach used to compute GPS-based orbits for altimeter calibration activities at Harvest.

TOPEX/Poseidon carries a GPS Demonstration Receiver (GPSDR) capable of tracking up to 6 GPS spacecraft simultaneously. Observations collected concurrently on the spacecraft and at 11-13 globally distributed ground sites are used to determine the orbits. Prior to launch, covariance analyses and simulations indicated that the reduced dynamic orbit determination approach described above will lead to the highest global rms accuracies (< 10 cm) for the radial height component of the orbits [Wu et al., 1991]. Post-launch analysis shows that actual performance, < 3 cm rms, far exceeds this expectations [Bertiger et at., this issue].

Since the flight receiver is not capable of tracking in a codeless mode, this level of accuracy will be achievable only when encryption of the precise ranging code (AS) is turned off. The TOPEX/Poseidon project had been guaranteed only 90 days worth of unencrypted data during the verification phase of the mission; however, up until the present time, AS has onty been activated occasionally, so more data has been obtained than anticipated.

TOPEX/Poseidon GPS orbits are computed at the Jet Propulsion Laboratory (JPL) using the GIPSY software. Arc lengths of 30 hours were considered to be reasonable compromise between orbit error and.

computational efficiency. GPS orbits have been obtained for most of the first 36 overflights of Harvest. Some data outages occurred when AS was on, the GPSDR was in a re-set mode, and the spacecraft was in safe-hold.

5.4 Orbit *Comparisons*

Figure 5.2 shows a comparison between the orbital heights obtained from JPL GPS, JPL SAO, and CSR Tuned orbits using the GSFC POE as a reference. The mean differences are -0.6 $\pm$1.6 cm, -1.4 $\pm$1.6 cm, and -1.3 $\pm$1.4 cm respectively. A mean difference on the order of -2 to -1CM may reflect the geographically correlated error (GCE) in JGM-2 at Harvest, which would be present in a long-arc dynamic orbit such as the POE [Christensen et al., 1994]. The GPS and SAO techniques are basically geometrical in the nature and should thereby have little *or no* GCE. It is expected that the CSR tuned gravity model would introduce an even smaller GCE than the JGM-2 model,

These results demonstrate that our knowledge of the orbital heights at Harvest far exceeds our pm-launch expectations (see Section 3). The fact that we obtain consistency on the order of a 1-2 cm rms with three independent orbits is testimony to the outstanding achievements of the TOPEX/Poseidon POD team. Note that none of the orbits show a significant secular trend relative to the POE. Clearly, any *one* of these sets of ephemerides can be considered to be representative of the orbit at tea.

6. TROPOSPHERIC PATH DELAY

The proximity of Harvest platform to the California coastline (- 11 km) resulted in the requirement of an independent determination of the wet tropospheric range correction for path delay (PD) applicable to the altimeter measurements over the verification site. The TOPEX/Poseidon Microwave Radiometer (TMR), which provides open-ocean path delay measurements over a -40 km footprint, is subject to land contamination effects at Harvest, and the accuracy of extrapolating the approaching TMR measurements to the Harvest position was undetermined prior to launch. In addition, previous comparisons between path delays measured at Harvest and path delays determined from the Vandenberg Air Force Base radiosonde data (- 10 km inland) indicated that large cross-coastal gradients in vapor burden can occur [Ruf and Keihm, 1990].

6.1 Upward-Looking Water Vapor Radiometer

As stated above, a ground-based water vapor radiometer (WVR) was deployed at the Harvest site prior to TOPEX/Poseidon launch to provide co-located path delay measurements for the altimeter calibration effort [Keihm et af., 1993a], The WVR is a JPL J- series three-channel instrument which measures sky brightness temperatures at 20.7, 22.2, and 31.4 GHz with half-power beam widths of ~ 9, 7, and *6* degrees respectively.

During the verification phase, the WVR operated in a continuous Yipping curve' mode which provided gain monitoring and zenith brightness temperature measurements every 90 seconds [Keihm et at., 1993b]. The absolute calibration accuracy is - 0.5 K for each channel, which translates to a path delay retrieval uncertainty of 0.3 cm due to instrument effects alone [Keihm, 1991]. The dominant retrieval error is due to a -5% uncertainty in the 22.235 GHz water vapor absorption model which links the brightness temperature measurements to vapor abundance. However, since the same absorption model is assumed in both the TMR and WVR retrieval algorithms, this error will be shared by both measurements.

62 *TMR, WVR, and Radiosonde Comparisons*

Due to the high wind and salt air conditions at the platform, the WVR experienced a number of hardware problems that do not normally occur in less adverse environments. As a result, for five of the first thirty cycle overpasses (cycles 9, 13, 14, 21, and 28), no WVR data was obtained, and the required path delay corrections for altimeter verification were obtained from the TMR measurements at a distance of ~ 30 km up-track from Harvest. The accuracy of the TMR extrapolation can be examined by comparing TMR path delay measurements to the WVR values for the 24 overpasses which included both TMR and valid WVR data. The cycle-to-cycle results are shown in Figure 6.1 with the TMR values representing measurements 30 km up-track from the platform. Also shown in Figure 6.1 are path delays computed from Vandenberg radiosonde data which have been interpolated (over 12 hour intervals) to the overpass time.

Note that, in general, all three path delay measurements show the same cycle-to-cycle variations, with nearly identical mean values and most differences are at the 2 cm level or less. The exceptions are cycles 7 and 18 for which the WVR measurement exceeds both the TMR and radiosonde values by 5-6 cm. The cause for the large discrepancies has not been identified. Both overpasses occurred under aloud free conditions. One possibility is the presence of condensation on the WVR teflon horn cover or reflector. However, since the WVR operated unattended, the condition of the surface covers can not be verified. Since the Vandenberg radiosonde results for these cycles agree much more closely with the TMR results, we have utilized the extrapolated TMR PD values for these cycles in the altimeter bias analysis. For the remainder of the cycles for which WVR data were available, either the WVR or TMR measurements can be used in the closure analysis since they both represent the range correction directly over the platform. For the cycles for which the WVR was inoperative, the TMR results 30 km up track should be adequate.

An estimate of the error due to the 30 km separation is illustrated by consideration of the expected decorrelation in path delay over a 30 km distance. Analysis of extensive TMR open-ocean data indicates that the expected PD differences over 30 km are in the range 0.5-0.7 cm [Keihm et al., 1993b]. This value can be checked for the Harvest region by calculating rrns residual differences between the three sources of path delay measurement at Harvest, Figure 6.2 shows scatter plots of the TMR- and radiosonde-derived path delays versus the WVR value

at Harvest, omitting the cycle 7 and 18 "outliers". Note that the TMR and WVR data show the best agreement with an rms difference of 1.07 cm. This value should represent the orthogonal sum of the individual measurement errors and the 30 km decorrelation error. Since both the WVR and TMR algorithms use the same model for vapor absorption, onty instrument calibration and inherent retrieval errors contribute to the measurement uncertainties. For the WVR, the measurement error is -0,5 cm [Gary et al., 1985]. For the TMR, again neglecting the vapor absorption model uncertainty, the measurement error is -0.9 cm [Keihm et al., 1993a], If we assume the 30 km decorrelation error is 0.6 cm, then the orthogonal error sum is 1.19 cm, consistent with the observed TMR/WVR residual difference. A similar analysis for the WVR/Vandenberg and TMR/Vandenberg comparisons, including the dominant error due to the necessary time interpolation of the radiosonde data, indicates that the larger rms differences are reasonable, especially when considering the expected larger decorrelations at the coastline transition.

6.3 *Troposphere Calibration Results*

In summary, with the exception of the cycle 7, 9, 13, 14, 18, 21, and 29 overpasses, the platform WVR or TMR path delay measurements can be used in the altimeter bias analysis. For the conditions prevalent for cycles 1-30 (average PO ~ 10 cm), the estimated WVR wet troposphere range correction accuracy is 0.65 cm. This value includes the vapor absorption model uncertainty, instrument errors, and a small error contribution due to the difference in air mass sampled between the WVR and altimeter beams. For the remaining overpasses, the 30 km displaced TMR path delay measurements can be utilized. For these cases, the estimated error for the altimeter tropospheric range correction at Harvest is 1.34 cm, obtained from the orthogonal sum of the open ocean TMR error of 1,2 cm [Keihm et al., 1993b] and the estimated 30 km decorrelation error of 0.6 cm.

7. IONOSPHERIC PATH DELAY

As part of the TOPEX/Poseidon altimeter verification effort, GPS-based ionospheric calibrations were produced for the TOPEX/Poseidon over-flights of the Harvest oil platform in order to provide an independent measure of the ionosphere that could be compared to the ionosphere measurements from the dual-frequency altimeter and DORIS. The ionosphere calibrations were generated using GPS data from a TurboRogue GPS receiver which has been in place at the Harvest oil platform since September, 1992.

GPS-based calibrations of the ionosphere directly overhead (zenith) the Harvest platform were generated for the exact instants that TOPEX/Poseidon flies over the platform. The over-flights repeat approximately every 10 days. For each over-flight, the instantaneous GPS-derived ionospheric delay looking straight up from the receiver on the platform can be compared to the ionospheric delay measured by the downward-looking

dud-frequency altimeter. This is a limited comparison since it yields only one number for each cycle, but by looking at many cycles one can check for systematic biases in the altimeter ionosphere measurements.

The verification team used an existing GPS-based ionosphere calibration system, developed at JPL, to produce the calibrations. A complete description of the models used to generate ionosphere calibrations from single-site GPS data is beyond the scope of this paper, but the basic technical issues will be summarized below.

7.1 *TEC Measurements Derived from GPS*

The GPS satellites provide both pseudorange and carrier phase data-types at two frequencies, L_1 and L_2, and both data-types provide a measure of the ionosphere. Unfortunately, line-of-sight total electron content (TEC) measurements computed by differencing dual-frequency GPS delays are corrupted by instrumental biases in both the receiver and GPS satellite transmitters. The line-of-sight differential delay for a receiver looking at a GPS satellite can be modeled by the following expression:

$$t^{LOS} = b_r + b_s + TEC^{LOS} + \text{noise (mostly multipath)} \qquad (7.1)$$

where t^{LOS} is the line-of-sight (LOS) differential delay, b_r is the receiver instrumental bias, b_s is the satellite instrumental bias, and TEC^{LOS} is the line-of-sight TEC. The TEC is usually expressed in TEC units (1 TECU = 10^{17} electrons/meter^2). One nanosecond of differential delay at L band corresponds to 2.85 TECU.

The receiver instrumental bias can be as large as&) TECU and therefore must be taken into account if one is to obtain accurate TEC measurements from GPS. The receiver bias for some GPS receivers can be calibrated directly with an accuracy of approximately 0.6 TECU [Wilson and Mannucci, 1993], but unfortunately a direct hardware calibration is not currently available for the TurboRouge receiver at Harvest. Therefore, the receiver bias must be estimated indirectly. The simplest technique is to collocate the receiver with a calibrated Rogue receiver. Differencing the pseudorange observables from the two receivers provides a measure of the difference of the two receiver biases.

The GPS satellite instrumental biases cannot be calibrated directly, but instead must be estimated from the GPS data itself by using a model of the ionosphere. The biases can be estimated separately since they are independent of the elevation angle while the TEC is elevation-dependent. Current estimates indicate that the GPS satellite biases can be as large as&9 TECU so the satellite biases also cannot be ignored if one is to obtain TEC more accurate than 10 TECU. JPL has developed a simple ionosphere model and estimation software which can produce global TEC maps using GPS data from a world-wide network of 30-40 GPS receivers and simultaneously solve for the satellite biases [Mannucci et al., 1993], The satellite biases can also be estimated from single-site fits, but with much less accuracy than the global fits (3-5 TECU instead of 2 TECU). A complete discussion of the problem of estimating the instrumental biases appears in Wilson and Mannucci [1 993].

A conservative error budget for GPS-derived TEC maps is shown in Table 7.1 (adapted from Wilson and Mannucci [1993]). The current global ionospheric monitoring software yields satellite biases with an estimated accuracy of 1 *A-2.8* TECU, which results in a total LOS TEC error of 1.6-3.2 TECU. This is the uncertainty in the raw LOS TEC observable one can derive from GPS data. In order to map the TEC measurements to an arbitrary LOS, the TEC data must be fit to a model of the ionosphere. This mapping process introduces an additional error, which is a function of the distance between the desired LOS and the nearest (in space and time) GPS measurements. The total error budget for mapped zenith TEC is estimated at 2-6 TECU or 0,4-1.3 cm at Ku band (1 cm at Ku band equals 4.59 TECU).

7.2 Ionosphere Model

The density of electrons in the ionosphere is largely concentrated in the F layer at an altitude of 250-450 km, so it is a reasonable approximation to model the ionosphere as a thin spherical shell, The particular spherical shell model used in our ionosphere calibration *system is* described in detail in Lanyi and Roth [1988]. Briefly, the vertical total electron content is approximated by a spherical shell with infinitesimal thickness at a fixed height of 350 km. The TEC is also assumed to be constant in time for several hours in a reference frame fixed to the Earth-Sun axis. Since the solar extreme ultraviolet flux is the primary physical driver of the ionization, this is a reasonable approximation. The intersection of the LOS from the receiver to the GPS satellite with the spherical shell defines a shell latitude and longitude, where the zero of shell longitude points toward the Sun, The LOS TEC is converted to an equivalent vertical TEC at the shell intersect point by using an elevation mapping function M(E), which is the simple geometric slant ratio at the shell height (h):

$$M(E) = \{1 - [\mathrm{Cos}(E)/(1 + h/R)]^2\}^{-1/2} \qquad (7s2)$$

where E is the elevation and R is the radius of the earth, M(E) ranges from 1 at zenith to a little over 3 at low elevation.

Once the TEC measurements have been mapped to vertical, the vertical TEC on the Sun-fixed shell can be modeled by fitting several hours of data to a two-dimensional polynomial in shell latitude and longitude. Figure 7.1 shows the coverage on the shell for a typical fit using a two hour span of GPS data: one hour on either side of the cycle 23 over-flight time, 23:06:46 UT on 93/04/40. The curved lines show the shell intersects for the 5 GPS satellites, The shell intersect of Harvest zenith at 23:06:46 UT is marked with a triangle symbol. The TEC data that are near the desired LOS on the shell (and near in time) are weighted more heavily so the frt is optimized for the desired point of calibration. The final calibration is then generated by evaluating the optimized polynomial at the appropriate shell latitude and longitude.

7.3 *Ionosphere Calibration Results*

The instrumental bias for the TurboRogue receiver at Harvest has been indirectly calibrated by comparing it with a calibrated Rogue receiver at Vandenberg Air Force Base which is only 10 km away from Harvest, The Harvest receiver can be roughly calibrated by differencing the Vandenberg and Harvest GPS-derived TEC data, Such an analysis yields an estimate for the Harvest receiver bias of -10.3 $\pm$1.7 TECU. The larger uncertainty in the receiver bias (due to indirect calibration on a non-zero baseline) results in a larger uncertainty in the absolute level of the resulting ionosphere calibrations.

To verify that the estimated receiver bias for Harvest was correct, the ionosphere calibrations for several over-flights were produced using GPS data not from Harvest, but instead from directly calibrated Rogue receivers at Vandenberg, Goldstone, and JPL. Since the baselines are so short, all the receivers provide adequate shell coverage to calibrate the Harvest zenith point. In all cases, the calibrations from the four sites agreed to within 2-3 TECU.

Ionosphere calibrations were generated using GPS data from the Harvest receiver for 19 over-flights. For all of these calibrations, the Harvest receiver bias was set to -10.3 TECU and the best estimates of the satellite biases available from the global ionospheric monitoring software were used. Figure 7.2 is a plot comparing the GPS-based ionosphere calibrations to the ionosphere measurements from the TOPEX/Poseidon dual-frequency altimeter. (The DORIS ionosphere value was substituted for 5 over-flights for which the altimeter value was not available.) The values are expressed in units of cm at Ku band. The differences (Harvest GPS minus TOPEX/Poseidon) for the 19 over-flights have a mean of -0.01 cm and a standard deviation of 0.9 cm. Excluding the 5 DORIS points, the differences have a mean of -0.4 cm and a standard deviation of 0,7 cm, so on average the GPS values are slightly lower than the altimeter values. The GPS values are expected to be systematically higher than the TOPEX/Poseidon values since the GPS measurements include the tail of the ionosphere (0.2-1.0 cm) above TOPEX/Poseidon's orbital attitude. Although the limited statistics prevent a definitive concision, this comparison indicates that systematic biases in the GPS and dual-frequency altimeter measurements of (absolute) ionospheric delay are small, certainly below the level of 1 cm.

9. TIDE GAUGE DATA ANALYSIS

Following the analysis of Parke et al. [1994], tide gauge data gathered during the first 36 cycles of the mission were examined for internal consistency. For the closure analysis, the average sea level for most of the overflights was obtained by averaging the high-rate data over 60 to 900 second intervals centered at tea. it was found that the mean was not particularly sensitive to the averaging period. The low-rate NGWLMS data was linearly interpolated to tea. Using the acoustical tide gauge as a reference, it was found that the bubbler and

transducer systems overestimated sea level by 1.3 ±2.7 cm and 0.7 ±2.3 cm respectively.

A detailed analysis of the time series suggested that the discrepancies were to some extent attributable to SWH. Therefore, if the wave height dependence for one of the tide gauges were known, it would be possible to calibrate the other two, An empirical sea-state correction for each of the three tide gauges was developed by comparing measured sea level with that predicted by a coastal tide model derived from TOPEX/Poseidon data [Parke et al., l994]. After applying the empirical corrections to the data, the bubbler and transducer gauges were no longer biased relative to the acoustical tide gauge, and the standard deviations were reduced to ±2.0 and ±2.1 cm respectively (see Figure 8.1).

9. CLOSURE ANALYSIS

The closure equation used for the analysis presented in this paper can be expressed as (see Figure 9.1)

$$\text{Bias} = H_{sat} - H_{gps} - H_{gp} - H_{pt} - H_{tg} - H_{gg} - R_{gdr} \quad (9.1)$$

Where H_{sat} is the height of the orbit and H_{gps} is the height of the GPS monument at Harvest relative to the ellipsoid, which includes corrections for the solid-earth-tide and the pole-tide. H_{gp} and H_{pt} are determined from a local survey that ties the *GPS* monument to the tide gauge monument, H_{tg} is the tide gauge measurement at tea, which is measured positive downward, (Note that no correction for the ocean-tide is necessary since it is observed by both the altimeter and in situ system and thereby cancel out of the closure equation.) H_{gg} is the geoid gradient correction. In keeping with the GDR notations, R_{gdr} is the "true" altitude as observed by TOPEX/Poseidon, defined by,

$$R_{gdr} = R_{measured} + R_{embias} + R_{iono} + R_{wet} + R_{dry} \quad (9.2)$$

Where $R_{measured}$ is the altitude prior to media corrections for EM-bias (R_{embias}), ionospheric path delay (R_{iono}), wet tropospheric path delay (R_{wet}), and dry tropospheric path delay (R_{dry}).

The baseline approach adopted for this analysis is to use the Geophysical Data Records (GDRs) for the altimetric component, GPS ephemerides for the orbit component, and the NOAA NGWLMS tide gauge for the sea level component of the analysis, The previous sections have shown that, in a statistical sense, these data sets are *representative* of the in situ data sets gathered at Harvest. That is, comparable results can be obtained by choosing virtually any combination of the TOPEX/Poseidon and in situ data sets described in this paper.

9.1 *Interpolation of GDR Data*

The GDR provides altimeter and sea surface height (SSH) data at the rate of -1 Hz and -10 Hz and the remaining ancillary parameters at the rate of ~1 Hz. [Callahan, 1993], Smoothing the data in the vicinity of the time-of-closest approach (tea) to Harvest is necessary to minimize errors introduced by system noise. Elementary least-squares fits to low-order polynomials were used to fitter the data. The polynomial coefficients were then used to interpolate and, in some cases, extrapolate the data to tea. Using the spectral content of the data as a guide, the time span and order of the polynomial were varied until we found a regime that introduced the 'least change" in the interpolated parameter. Care was taken to ensure that no spurious signals resulting from land contamination were present in the fitted data span.

An objective analysis of the residuals obtained after performing the polynomial fits were used to judge the quality of the data, and thereby the quality of each pass. On occasion, it was necessary to remove blunder-points from the data sets. Subjective editing based on data flags proved to be too conservative because passes that survived the objective analysis were sometimes flagged. It was concluded that the flags are very useful for editing the global data set; however, objective analysis is advisable when examining altimeter data atong coastal margins.

Raw altimeter data provided at the -10 Hz rate were fit with a 5th order polynomial over a time span of -1 0s to +1s relative to tea. Consistent with the notation adopted for the GDR, the 'raw" altimeter data is quantity $R_{measured}$ defined by the dosure equation given above. Smoothed values for the media corrections, described below, are later applied to obtain the corrected altimeter data (see Equation 9.2). Prior to launch, we did not expect to find high quality altimeter data much beyond the tea. However, a detailed analysis of all of the passes considered in this analysis revealed that the ALT remained in ocean-track mode up to 1-to-2 kilometers of shore, with no obvious indications of land contamination. This is probably due to the fact that the palisades along the coast of Point Conception are out of range of the Ku-band altimeter until land occupies a significant portion of the beam-limited footprint. The rms residuals ranged from -2.4 to -6.2 cm for the passes considered in this analysis.

The -1 Hz TMR path delay data were fit with a 1st order (linear) *polynomial over* a time span of -15s to. 5s relative to tea. The rms residuals for the fit were typically less the 0.5 cm. To avoid the effects of land contamination, the value of the polynomial at -5s, approximately 30 km *from* Harvest, was applied to the altimeter data at Harvest. (See Section 6 for a more detailed discussion of the extrapolation of TMR data.) The dry tropospheric correction was obtained by interpolating *between* the two points on either side of tea.

The ~1 Hz ALT and DORIS ionosphere data were fit with a 4th order polynomial over a time span of -30s to -1s relative to tea. The value of the polynomial at -1s was applied to the altimeter data at Harvest. The rms residuals for the fit were typically less than 1,0 cm. The time span is considered to be optimum for smoothing because, as pointed out by Imel [this issue], the ionospheric path delay is virtually uncorrelated over distance of 100-200 km. The data span was terminated at -1s for the ALT since a detailed analysis of the residuals for almost all passes revealed a systematic trend in the data beyond this point. It is suspected that this is due to land contamination at C-band, which has a larger beam-limited footprint than the Ku-band channel.

The -1 Hz EM-bias corrections at Ku-band were fit with a 3rd order polynomial over a time span of -10s

to +1.1s relative to tea. The interpolated value of the polynomial at tca was applied to the altimeter data at Harvest. The rms residuals for the fit were typically less than 0.3 cm. The time span was extended to +1 .1s to ensure that at least one data point after tca would be included in the fit. The NASA algorithm for EM-bias was used for both the ALT and SSALT overflights. It was necessary to apply an additional correction of -2,3% of SWH to the SSALT data to account for sea-state bias [Shum et al., this issue],

The solid-earth-tide and pole-tide corrections were obtained by interpolating between the two -1 Hz points on either side of tea. This is quite acceptable since they are derived from smoothly varying models that can be interpolated very accurately.

Two additional parameter, SWH and SSH, were fit to provide ancillary information that could be used to look for correlations in the altimeter bias estimates. The same strategies used to interpolate EM-bias and ALT data were used for SWH and SSH respectively.

92 *TCA, Reference Elllpsoid, and Geold Gradient*

The toe is determined by minimizing the length of the great-circle arc between the platform and the position of the satellite along the groundtrack, i.e. maximize

$$\mathrm{Cos}(d) = \mathrm{Sin}(t)\,\mathrm{Sin}(h) + \mathrm{Cos}(t)\mathrm{Cos}(h)\mathrm{Cos}(z) \qquad (8.3)$$

where d is the distance-of-closest- approach (dca), t is the latitude of TOP EX/Poseidon, h is the latitude of Harvest, and z is the longitudinal span between the satellite and the platform at a given time. The time at which d is minimized, which is determined using a golden-search procedure, is the tea. The latitude and longitude of Harvest are 34.470923?4 and 239.314155"E respectively. It was found that the various satellite ephemerides used for this analysis; SLR/DORIS long-arc (POES), SLR short-arc, and GPS all produced tca estimates that agree to better than 100us.

TOPEX/Poseidon actually measures geocentric sea level, but it is convenient to express it as height relative to the reference ellipsoid, i.e. SSH. (Because the reference ellipsoid is a well defined mathematical model, geocentric sea level and SSH are physically equivalent.) Consequently, the definition of the reference ellipsoid is central to the analysis of the altimeter data. For the work presented here, we use the standard model adopted for TOPEX/Poseidon, a_e = 8378.1383 km and I/f = 298.257, where a. is the semi-major axis of the equator and f is the Earth flattening.

Gradients in the sea surface piay an important role in satellite altimetry. As the groundtrack varies over a region, spatial variations in the sea surface manifest themselves as temporal variations in sea level. For this reason, the TOPEX/Poseidon groundtrack is onty allowed to vary by ± 1 km in the cross-track direction. Nevertheless, in some regions, erroneous signals on the order of 1 to 2 cm can be introduced by the sea surface

gradient. Apart from spatial and temporal variations in sea level due to ocean dynamics, the geoid closely' approximates the sea surface. Therefore, we examined the geoid gradients at Harvest in an attempt to minimize errors proportional to the dca. Based on a limited set of GeoSat and shipboard data, the cross-track geoid gradient at Harvest is estimated to be 0.8 cm/km, trending upward toward the northwest [Rapp (personal communication), 1993]. Efforts are currently underway to improve our knowledge of the geoid gradient at Harvest using TOPEX/Poseidon data.

9.3 *Results and Discussion*

Using the procedures and definitions described above, preliminary estimates for the mean bias of the ALT and the SSALT have been obtained using data gathered during the first 36 cycles of the mission. Data for 21 overflights of the ALT and 3 overflights of the SSALT were combined in accordance with the dosure equation (Equations 9.1 and 9.2) to obtain a bias estimate of -14.7 $\pm$2.1 cm for the ALT and +2.9 $\pm$2.4 cm for the SSALT (see Figure 9.2). These results are consistent with independent estimates for the relative bias between the two altimeters [Shum et al., this issue], [Nerem et at., this issue], and [Menard et al, this issue], The sign convention, is such that a correction to absolute sea level derived from the GDR altimeter data can be obtained by algebraically adding the bias to the data.

A weighted linear regression applied to the complete set of data indicates a secular trend in the ALT bias of 3.6&2.4 cm/yr. The weighting factor was based on the variance of the raw altimeter residuals plus an expected sea state variance proportional to 1 % of SWH for each pass. If data for the first 15 cycles is excluded from the analysis, the estimated slope is negligible. A candidate explanation is that this "drift" is introduced by an error in the in situ measurements of sea level that is proportional to sea state. A portion of this error may also be due to EM-bias. Other potential causes; such as, geoid gradient, platform subsidence, TMR drift, orbit drift, and pointing errors have been investigated and ruled-out. An extension of the time series for mis-closure is needed to better understand this trend, particularly into the '93-'94 winter season where the sea state is expected to be high.

The closure analysis indudes an independent assessment of in situ measurements of sea level, the radial component of the orbit, tropospheric path delay, and ionospheric path delay. Tide gauges at Harvest provide estimates of sea level with an uncertainty of $\pm$2.1 cm. The uncertainty in the radial component of the orbit is estimated to be $\pm$1.6 cm. In situ measurements of tropospheric path delay at Harvest compare to within $\pm$1.3 cm of the TMR, and in situ measurements of the ionospheric path delay compare to within -0.4 $\pm$0.7 cm of the dual-frequency ALT and 1.1 $\pm$0.6 cm of DORIS.

Acknowledgements: We wish to extend our thanks to Willy Bertiger, Steve DiNardo, Lw Fu, B. Gary, Joe Guinn, Mike Janssen, Chesly McColl, Rodriqo Ibanez-Meier, Ron Muellershoen, and Yvonne Vigue at the Jet Propulsion Laboratory for making this work possible. We also would like to acknowledge: Andy Marshall and Creston Martin at the Goddard Space Flight Center; Richard Eanes, John Ries, and Piter Visser at the University of Texas, Austin;

Jim Johnson, Dan Kubitschek, Jimmy LaMance, Cregg McLaughlin, and Jennifer Myrick at the University of Colorado, Boulder; R, Edwing, D, Jones, T. Mere, M, Moss, M. Sarrrarrt, H. Shih, and W. Stoney at NOAA/NOS; and Chris Ruf at the University of Pennsylvania for their contributions to this effort. The work described in this paper was carried out at the Jet Propulsion Laboratory, California Institute of Technology, under contract with the National Aeronautics and Space Administration.

References

Bertiger, W.I. et al., GPS precise tracking of TOPEX/Poseidon: Results and implications, *J. Geophys.* Rest (this issue), 1994.

Bonnefond P., P. Exertier, F. Barlier and Ph. Schaeffer, Regional verification results in the Mediterranean area, *J. Geophys. Res.*, (this issue), 1994.

Born, G. H., C. Wunsch and C.A. Yamarone, TOPEX: observing the oceans from space, *EOS Trans., AGU,* 65,433 434, 1984.

Boucher, C. and Z. Altamimi, ITRF91 and other realizations of the IERS Terrestrial Reference System for 1991,, */ERS Technical Note*, available from the Observatoire de Paris, 1991.

Boucher, C. and Z. Altamimi, ITRF92 and other realizations of the IERS Terrestrial Reference System for 1992, */ERS Technics/ Note,* available from the Observatoire de Paris, 1992.

Callahan, P., TOPEX/Poseidon project GDR user's handbook, JPL D-8944, rev A, 84 pp, *Available from Distributed Active Archive Center,* Jet Propulsion Lab. 300-319, 4800 Oak Grove Dr., Pasadena, CA 91109, 1993.

Christensen, E. J., L-L. Fu, and M .E. Parke, TOPEX/Poseidon altimeter, orbit, and sea level verification, *Proceedings of the* OCEANS*89 *Conference,* Seattle, *Washington, 1989.*

Christensen, E.J. and Y. Menard (editors), TOPEX/Poseidon joint verification plan, JPL Pub. 92-9, *Available from Technics/ Publications,* Jet Propulsion Lab. 111-141, 4800 Oak Grove Dr., Pasadena ,CA 91109, 1992.

Christensen, E. J., B.J. Haines, K.C. McColl, and R.S. Nerem, Observations of geographically correlated orbit errors for TOPEX/Poseidon using the Global Positioning System, *Geophys. Res. Let.*, (to appear), 1994.

Filloux, J. H., Pressure fluctuations on the open ocean floor over a broad frequency range: New program and early results, *J.* Phys. *Oceanography,* 10(12), 1959-1971, 1980.

Gary, B. L., S.J. Keihm and M.A. Janssen, Optimum strategies and performance for the remote sensing of path-delay using ground-based microwave radiometers, */EEE Trans. Geosci. Rem. Sensing,* GE-23, 479-484, 1985.

Gill, S. K., R.F. Edwing, D.F. Jones, T.N. Mere, M.A.K. Moss, M. Samant, H.H. Shih, and W.E. Stoney, NOAA/National Ocean Service platform Harvest: Preliminary results, *Mar. Geod., (to appear),* 1994.

Imel, D., Evaluation of the TOPEX/Poseidon dual-frequency ionosphere correction, *J.. Geophys. Res.*, (this issue), 1994.

Keihrn, S. J., Water vapor radiometer comparison experiment: Platteville, Colorado, March 1-14, 1991, *JPL Dec. No. D-8898,* 1991.

Keihm. S.J., M.A. Janssen and C.S. Ruf, TOPEX/Poseidon Microwave Radiometer (TMR): III. Wet troposphere range correction algorithm and pre-launch error budget, */EEE Geosci. Rem. Sensing,* (submitted August 30, 1993a).

Keihm, S. J,. N. Yamane, A. Tanner, R. Swindlehurst, S. Walter and R. Newsted, Water vapor radiometer measurements at Harvest platform, Harvest Report, *JPL Dec. No. D-xxxx,* (to appear), 1993b.

Kolenkiewicz, R. and C.F. Martin, SEASAT altimeter height calibration, *J. Geophys Res.* 95, 3189-3197, 1982.

Kubitschek, D. G., M.E. Parke, G.H. Born, J. Johnson, and C, McLaughlin, CU sea level system at platform Harvest, *Mar. Geod.*, (to appear), 1994.

Lanyi, G. and T. Roth, A comparison of mapped" and measured total ionospheric electron content using global positioning system and beacon satellite observations, *Radio Sci.*, **23** (4), 483492, 1988.

Mannucci, A.J., B.D. Wilson and C.D. Edwards, A new method for monitoring the Earth's ionospheric total electron content using the GPS global network, *Proceedings of the Institute of Navigation GPS-93, Salt* Lake City, Utah, September, 1993.

Menard, Y. et al., Poseidon altimeter bias, *J. Geophys. Res.*, (this issue), 1994.

Morris C, S., S.J. DiNardo, and E.J. Christensen, Overview of the TOPEX/Poseidon platform Harvest verification experiment, Mar. *Geod.*, (to appear), 1994.

Nerem, R. S., Gravity model development for TOPEX/Poseidon, by GSFC, UT, CNES, *J. Geopys. Res.*, (this issue), l994.

Nouel, F., Precise CNES orbits for TOPEX/Poseidon: Is reaching 2 cm still a challenge, *J. Geophys. Res., (this* issue), 1994.

Parke, M.E. and S.K. Gill, Platform harvest tide gage comparisons, *Mar. Geod., (to appear),* l994.

Purcell, G.H. et at., GPS measurements at platform Harvest, Mar. *Geod.,* (to appear), l994.

Ruf, C.S. and S.J. Keihm, D-series JPL water vapor radiometer: Instrument description, data quality, and platform capability, 1990 TOPEX/Poseidon Platform Experiment, *JPL Dec. No. xxxx*, l990.

Scharroo, R., K.F. Wakker, H. Overgaauw and H.A.C. Ambrosius, Some aspects of the ERS-1 radar altimeter calibration, presented at the *42nd Congress of the International Astronautical Federation*, Montreal, Canada, October 5-11, l991.

Shum, C.K. et al., *J. Geophys. Res.*, (this issue), 1994.

Tapley, B. D., J.C. Ries, G.W. Davis, R.J. Eanes, C.K. Shum, M.M. Watkins, J.A. Marshall, R.S. Nerem, B.H. Putney, S.M. Klosko, S.B. Luthcke, D. Pavlis, R.G. Williamson, and N.P. Zelensky, Precision orbit determination for TOPEX/Poseidon, *J. Geophys. Res., (this* issue), l994.

Tapley, B. D., M.M. Watkins, J.C. Ries, G.W. Davis, R.J. Eanes, S.R. Poole, H.J. Rim, B.E. Schutz, and C.K. Shum, The TEG-3 gravity model, *J. Geophys. Res.*, (to be submitted), l993.

Wakker, K.F., R, Scharroo, B. Overgaauw, R. NoOmen and B.AC. Abrosius, ERS-1 radar altimeter calibration results, presented at the *AGU/CGU/MSA Joint Spring Meeting,* Motreal, Canada, May 12-16, 1991.

White, N,J., R. Coleman and J.A. Church, A southern hemisphere verification for the TOPEX/Poseidon satellite altimeter mission, *J. Geophys. Res.*, (this issue), *1994.*

Williams, B. G., E.J. Christensen, D.N. Yuan, K.C. McColl and R.F. Sunseri, Short arc orbit determinations for altimeter calibration and validation on TOPEX/Poseidon, *Spaceflight Mech.: Advances in the Astronautical Sciences*, 82, 889-899, l993.

Wilson, B. D. and A J. Mannucci, Instrumental biases in ionospheric measurements derived from GPS data, *Proceedings of the Institute of Navigation GPS-93*, Salt *Lake* City, Utah, September, 1993.

Wu, S. C., T.P. Yunck and C.L. Thornton, Reduced-dynamic technique for precise orbit determination of low earth satellites, *J. Guid., Control and Dynamics, 14(1), 24-30, 1991.*

Yunck, T.P. and S.C. Wu, Non-dynamic decimeter tracking of Earth satellites using the Global Positioning System, *AIAA paper* 86-0404, *AIAA 24th Aerospace Sciences Meeting,* Reno, NV, Jan 1986.

Yunck, T. P., W.I. Bertiger, S.C. Wu, Y. Bar-Sever, E.J. Christensen, B.J. Haines, S.M. Lichten, R.J. Muellerschoen, Y. Vigue and P. Willis, First assessment of GPS-based reduced dynamic orbit determination on TOPEX/Poseidon, *Geophys. Res. Lett.*, (to appear), 1994.

Figure Captions

Figure 1.1: The concept of closure at platform Harvest. Sea level relative to the reference ellipsoid as measured by the altimeter is compared to that determined from the orbit height and a tide gauge at the platform. Note that the GPS receiver on the platform is used to tie the tide gauge to the reference ellipsoid.

Figure 2.1: The location of the NASA verification site off the coast of the California coast. The ticked line is the TOPEX/Poseidon groundtrack for ascending pass #43 and the circle illustrates the spatial dimensions at the site relative to an idealized altimeter footprint.

Figure 2.2: Location of the in situ insturments on platform Harvest.

Figure 4.1: Vertical component of the geodetic baseline from Qunicy to Harvest.

Figure 4.2: Geodetic height of the Harvest platform determined by GPS in ITRF91 coordinates relative to the TOPEX/Poseidon standard reference ellipsoid.

Figure 5,1: SLR viewing geometry for TOPEX/Poseidon ascending pass #43 over Harvest. Horizon-masks are cut-off at 15" elevation.

Figure 5.2: JPL GPS, JPL SAO, and CSR Tuned orbit height estimates for Harvest relative to the GSFC POE orbit height.

Figure 6.1: Time series of WVR, TMR, and Vandenberg radiosonde observations of wet tropospheric path delay for Harvest overflights.

Figure 6.2: Scatter plot of TMR and Vandenberg radiosonde observations vs. WVR observations of wet tropospheric path delay for Harvest overflights.

Figure 7.1: The shell geometry for the cycle 23 over-flight fit using two hours of GPS data. The Sun-fixed shell intersects are shown for the five GPS satellites. The triangle marks the Harvest zenith intersect at the time of the over-flight on 93/04/30 (23:06:46 UT). The final GPS ionosphere calibration value will be largely determined by the data for satellites 2 and 13.

Figure 7.2: Comparison of the two ionosphere measurements for 19 over-flights: Harvest GPS versus the TOPEX dual-frequency altimeter. The DORIS ionosphere was substituted for 5 over-flights for which the altimeter number was not available. The ionospheric delay is expressed in units of cm at Ku band.

Figure 8.1: Tide gauge sea level difference for Harvest overflights (with Parke correction)

Figure 9.1: Schematic for constituents of the closure equation.

Figure 9.2: TOPEX/Poseidon altimeter biases at platform Harvest based on: GPS orbits; NOAA/NOS tide gauge data (with Parke correction); ALT, SSALT, and TMR GDR data,

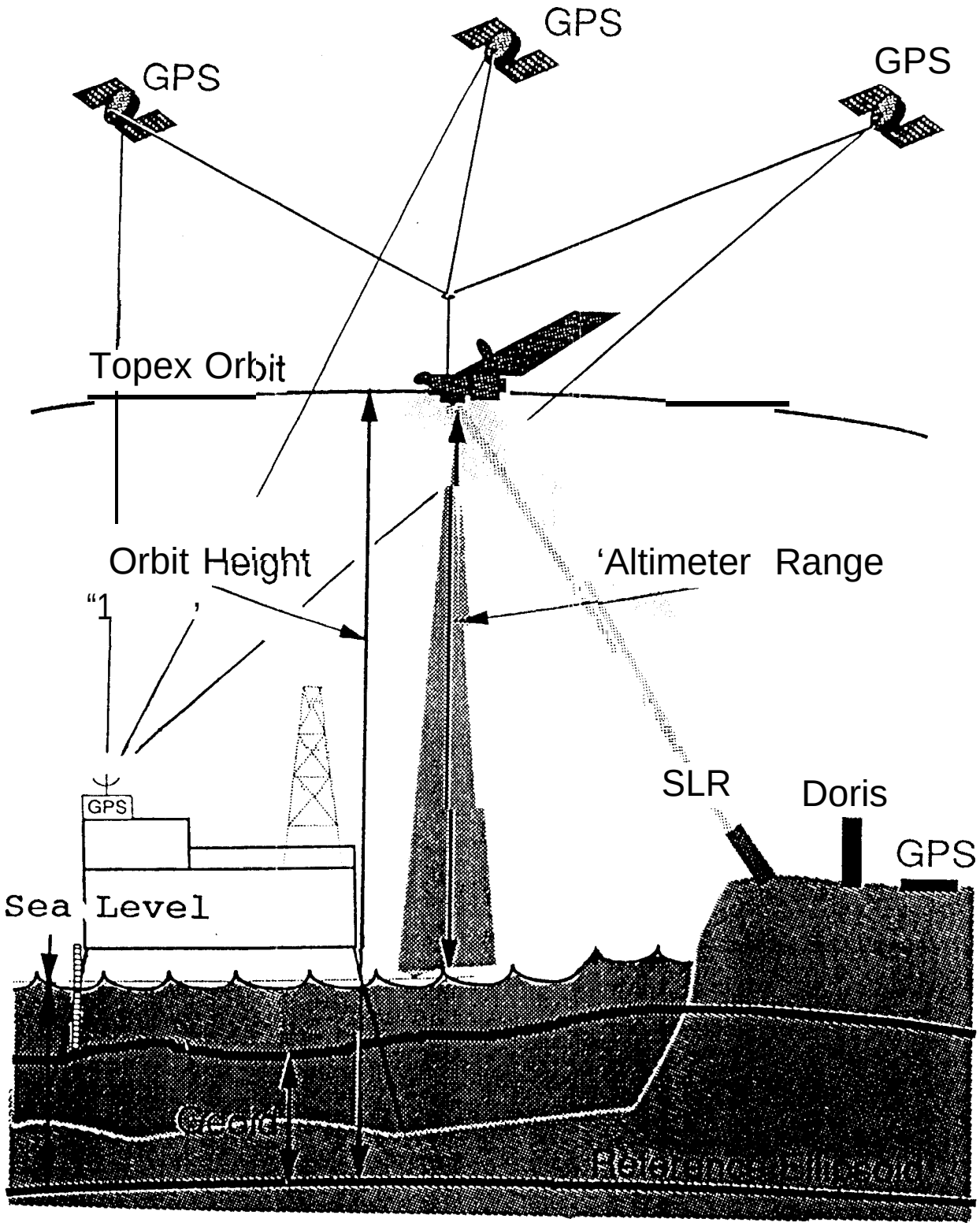
GPS
GPS
GPS
Topex Orbit
Orbit Height
'Altimeter Range
SLR
Doris
GPS
GPS
Sea Level

Figure 1.1

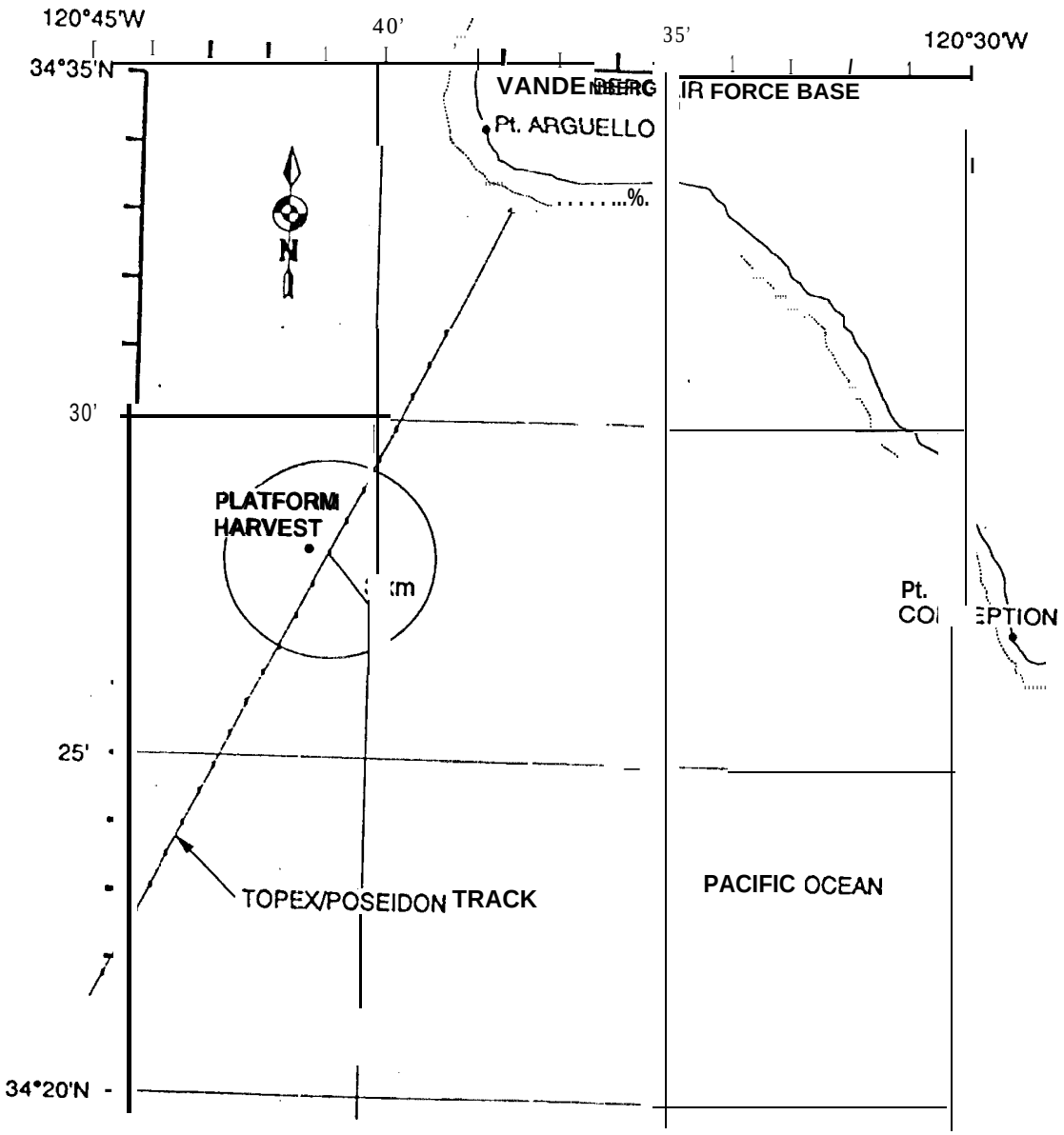
120°45'W
40'
35'
120°30'W
34°35'N
VANDE
IR FORCE BASE
Pt. ARGUELLO
N
30'
PLATFORM
HARVEST
Pt.
25'
PACIFIC OCEAN
TOPEX/POSEIDON TRACK
34°20'N

Figure 2.1

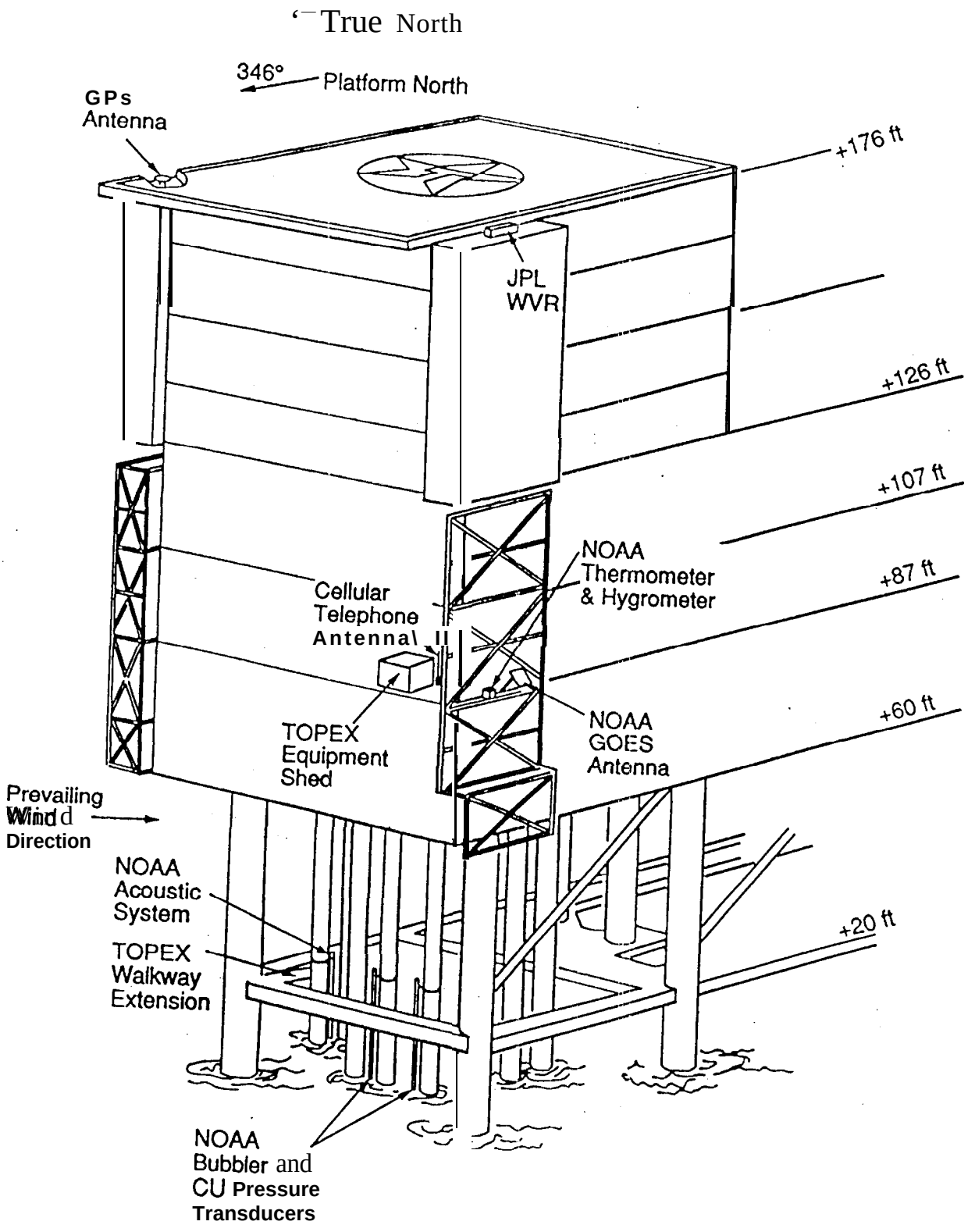
True North
346°
Platform North
GPs
Antenna
+176 ft
JPL
WVR
+126 ft
+107 ft
NOAA
Thermometer
& Hygrometer
+87 ft
Cellular
Telephone
Antenna
TOPEX
Equipment
Shed
NOAA
GOES
Antenna
+60 ft
Prevailing
Wind
Direction
NOAA
Acoustic
System
TOPEX
Walkway
Extension
+20 ft
NOAA
Bubbler and
CU Pressure
Transducers

Figure 2.2

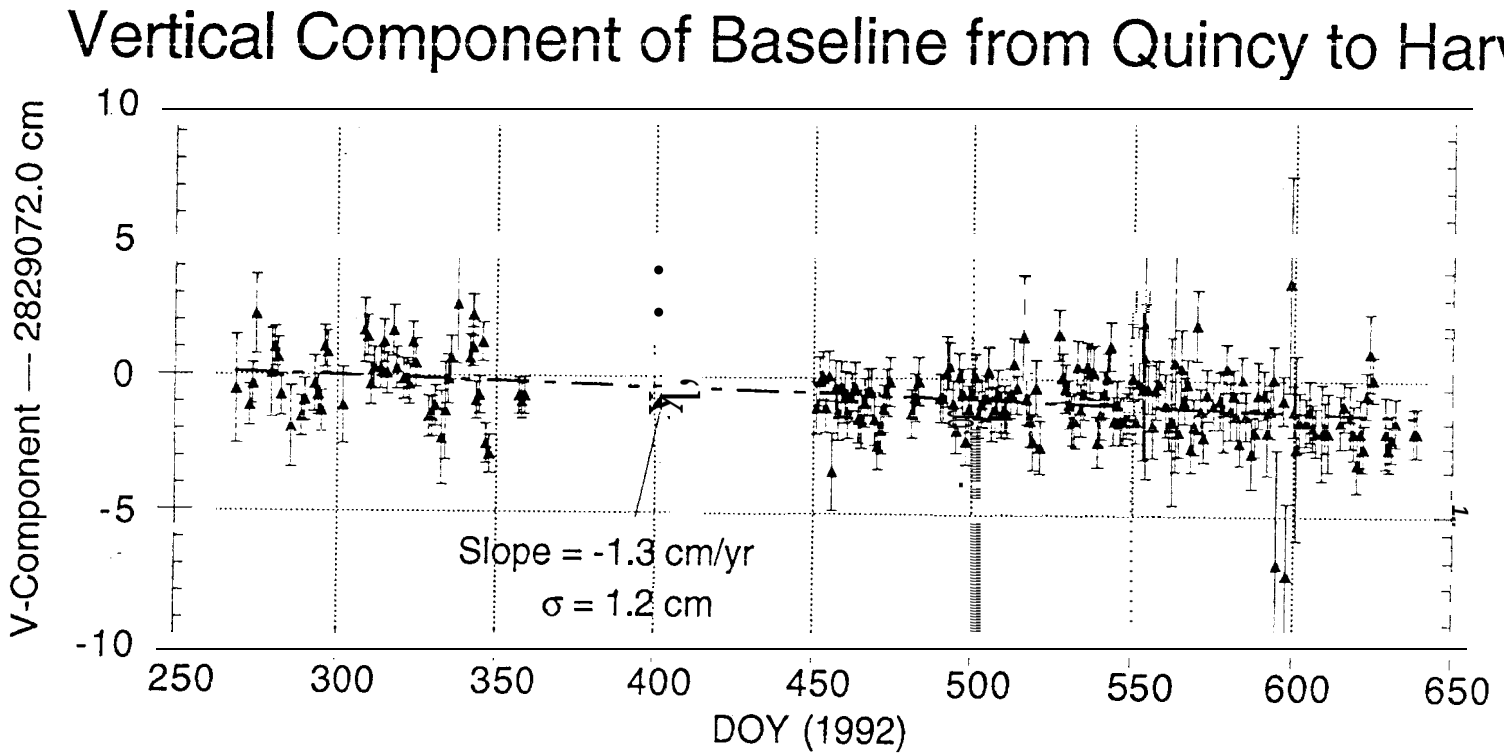
Vertical Component of Baseline from Quincy to Harvest
V-Component — 2829072.0 cm
10
5
0
-5
-10
250
300
350
400
450
500
550
600
650
DOY (1992)
Slope = -1.3 cm/yr
σ = 1.2 cm

Figure 4.1

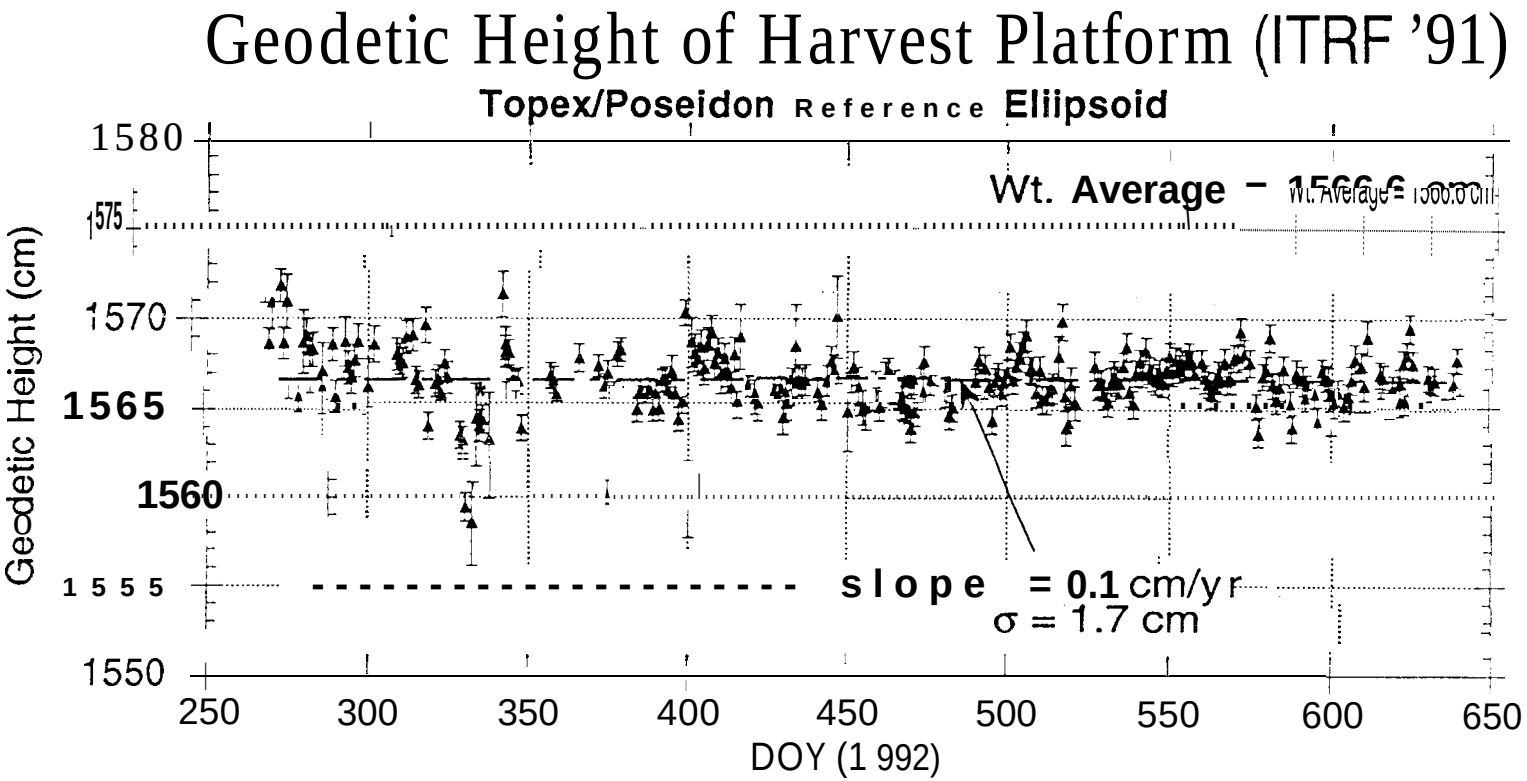
Geodetic Height of Harvest Platform (ITRF '91)
Topex/Poseidon Reference Eliipsoid
Wt. Average = 1566.6 cm
slope = 0.1 cm/yr
σ = 1.7 cm
Geodetic Height (cm)
1580
1575
1570
1565
1560
1555
1550
250
300
350
400
450
500
550
600
650
DOY (1 992)

Figure 4.2

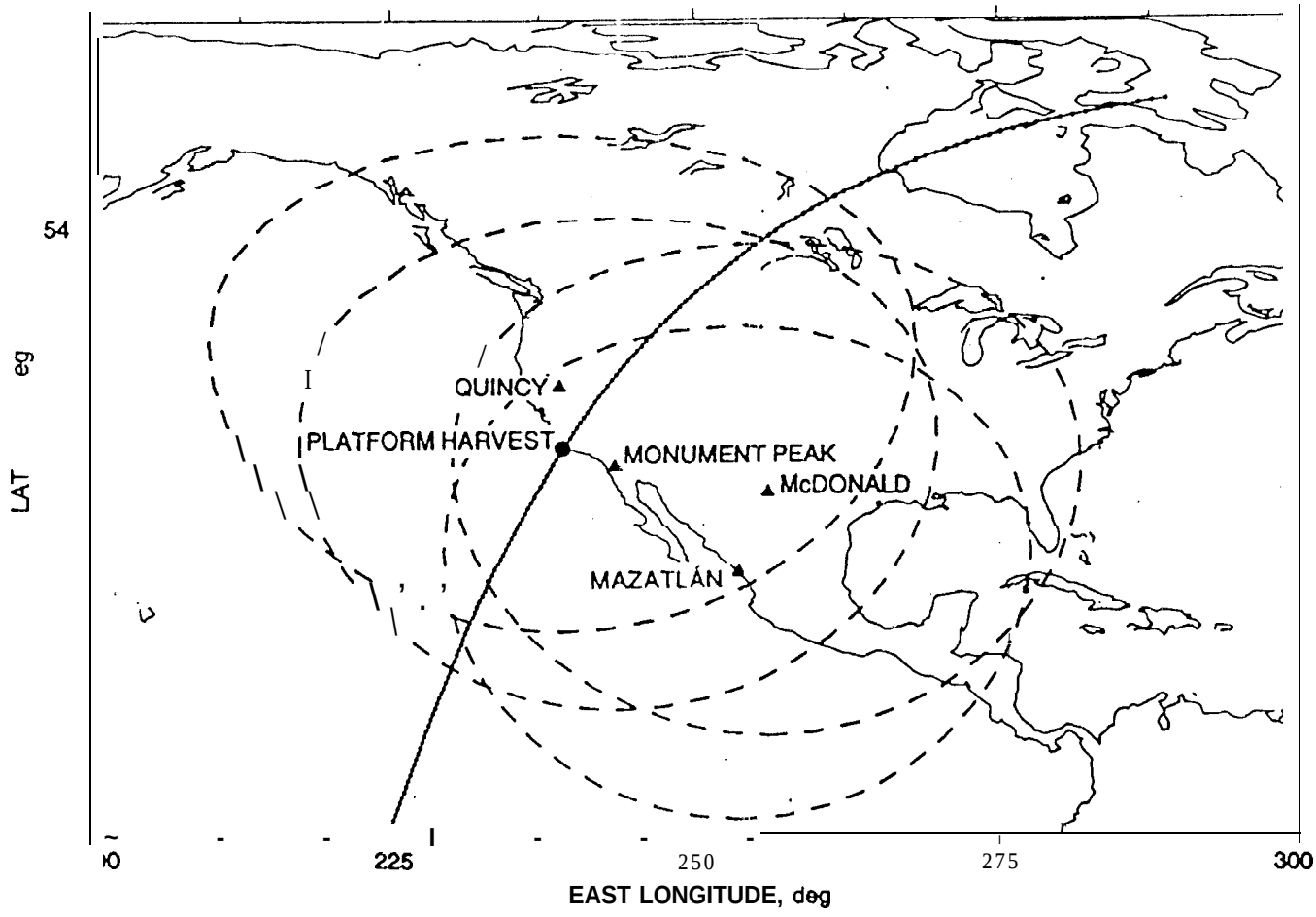
54
eg
LAT
QUINCY
PLATFORM HARVEST
MONUMENT PEAK
McDONALD
MAZATLÁN
225
250
275
300
EAST LONGITUDE, deg

Figure 5.1

Differences of Orbit Height Estimates for Harvest Overflights

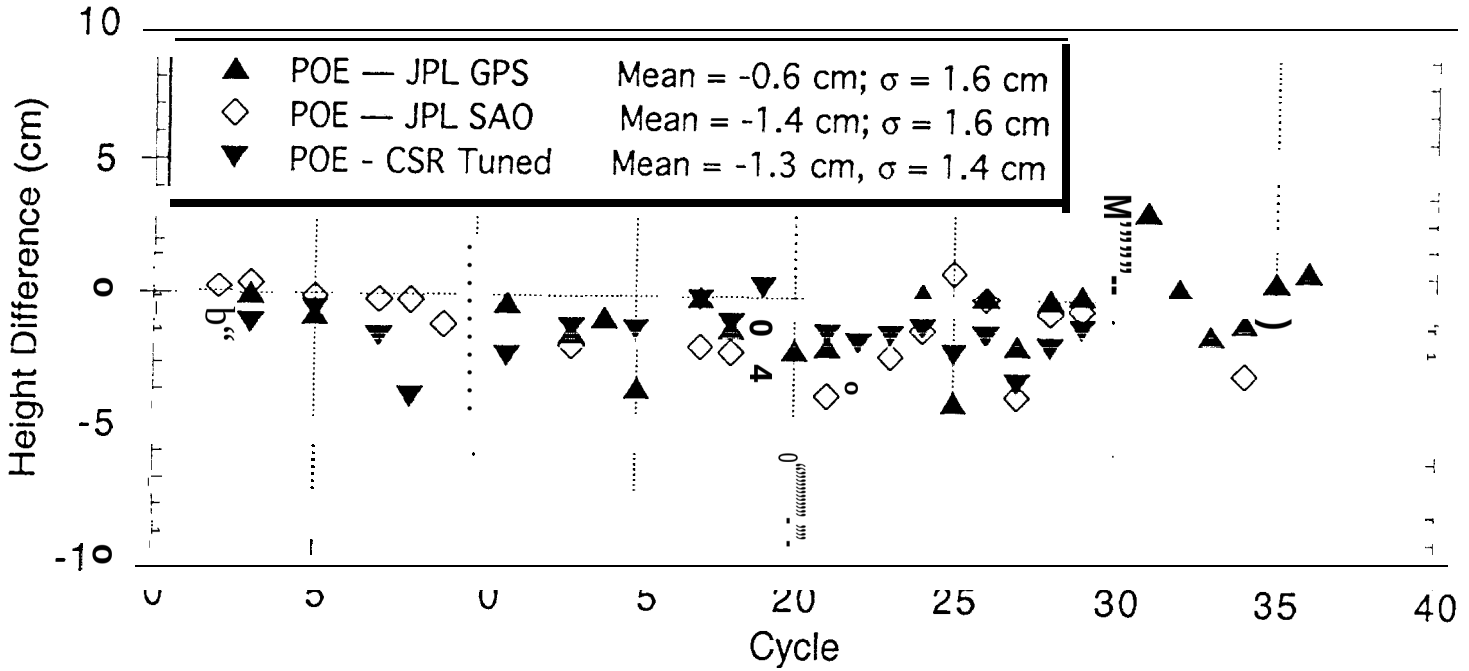

Figure 5.2

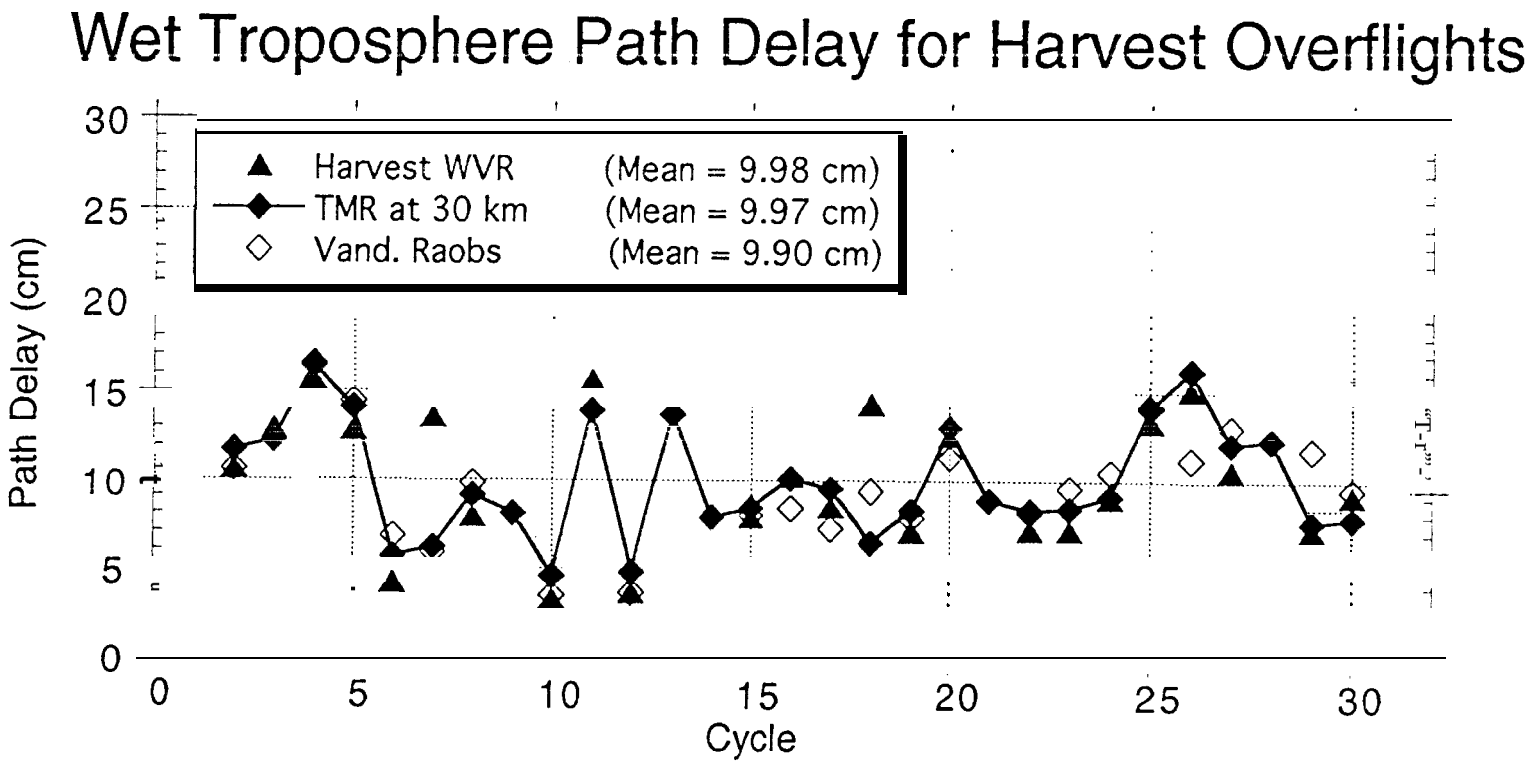
Wet Troposphere Path Delay for Harvest Overflights
Path Delay (cm)
30
25
20
15
10
5
0
Harvest WVR (Mean = 9.98 cm)
TMR at 30 km (Mean = 9.97 cm)
Vand. Raobs (Mean = 9.90 cm)
0
5
10
15
20
25
30
Cycle

Figure 6.1

Scatter Plot of Wet Troposphere Path Delays for Harvest Overflights

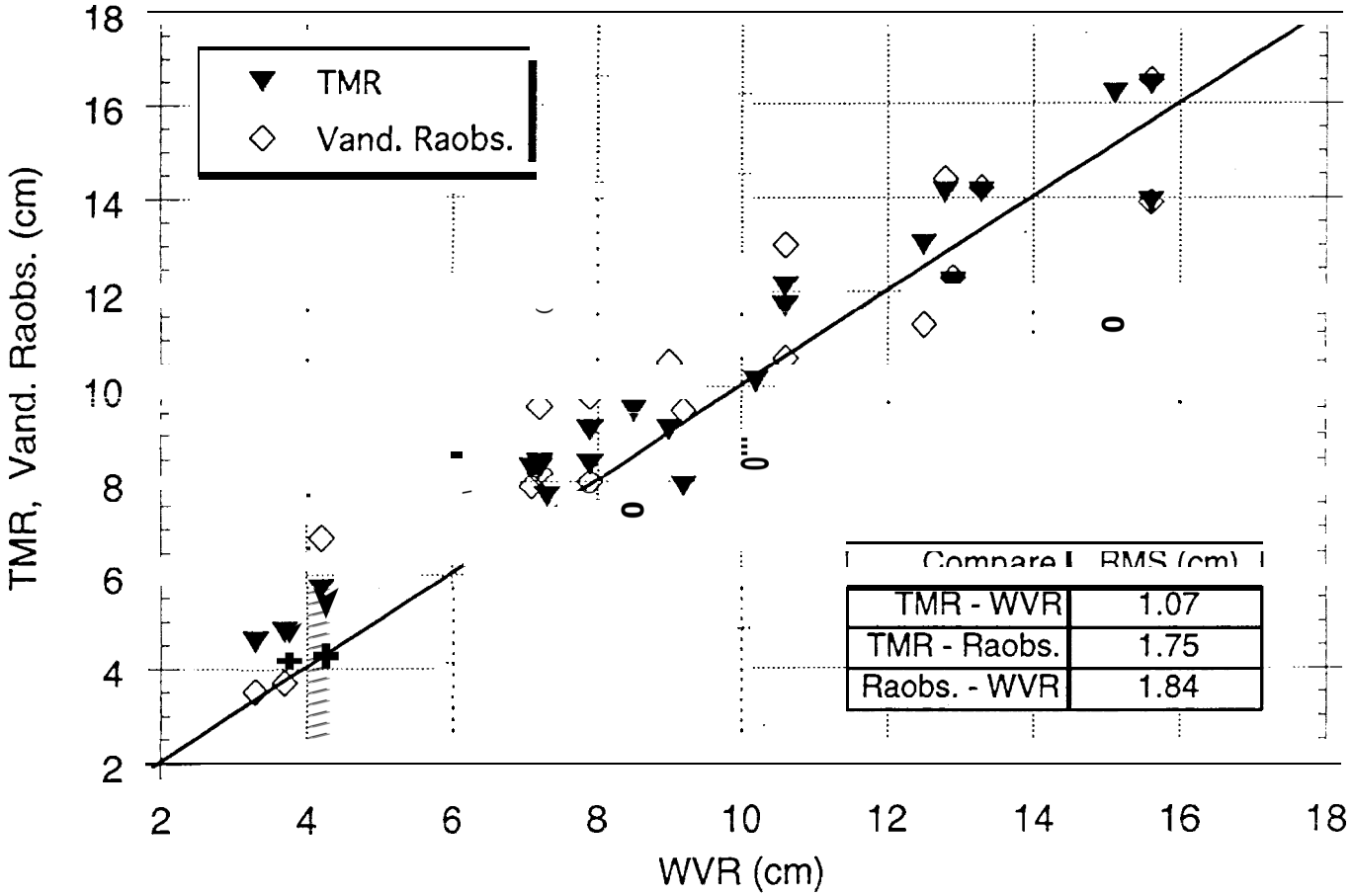

Figure 6.2

Sun-fixed shell "intersects. for a typical fit using 2 hours of **GPS** data

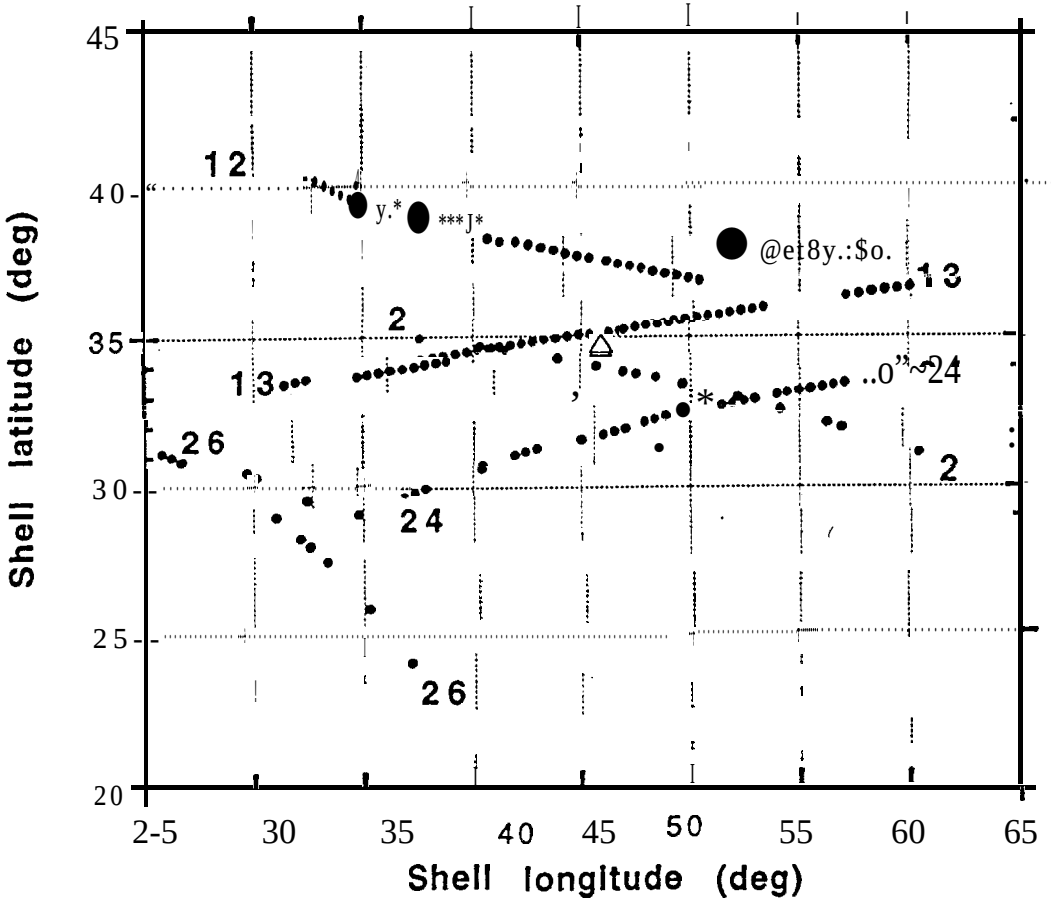

Figure 7.1

Ionosphere Path Delay for Harvest Overflights

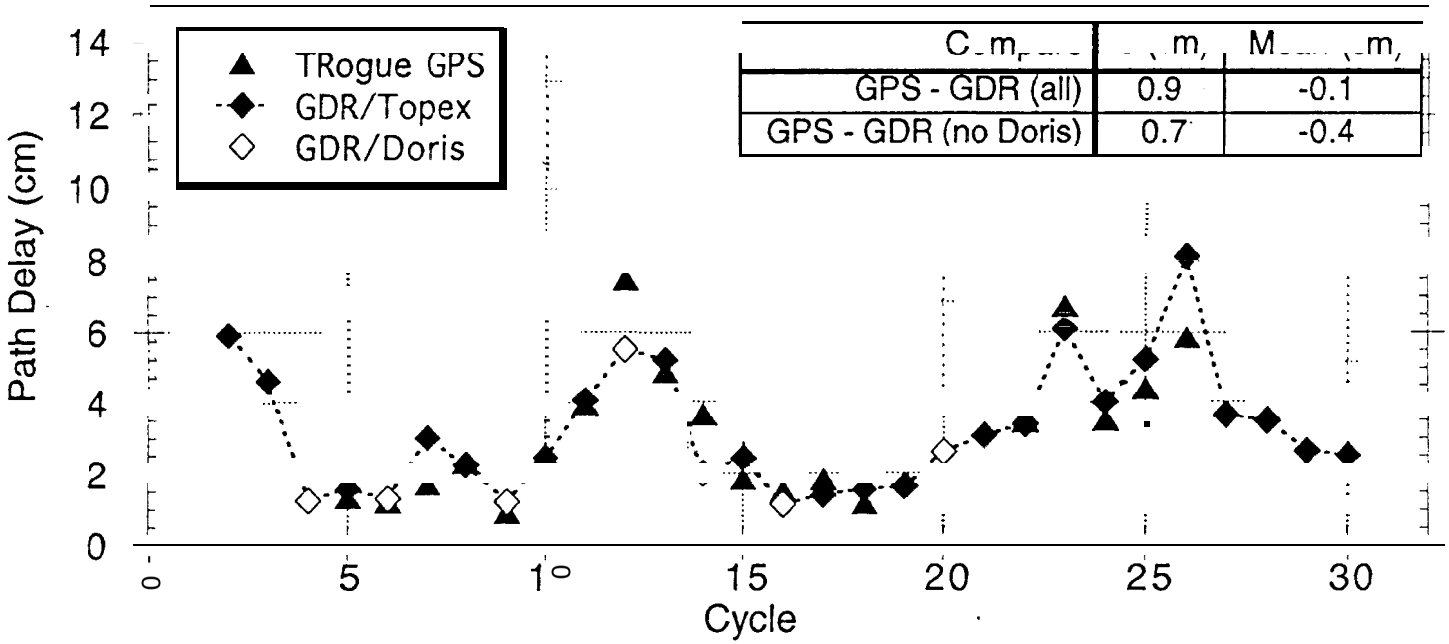

C_m_	_ _ m,	M_ _ _m,
GPS - GDR (all)	0.9	-0.1
GPS - GDR (no Doris)	0.7	-0.4

gu e 7.2

Tide Gauge Sea Level Differences for Harvest Overflights

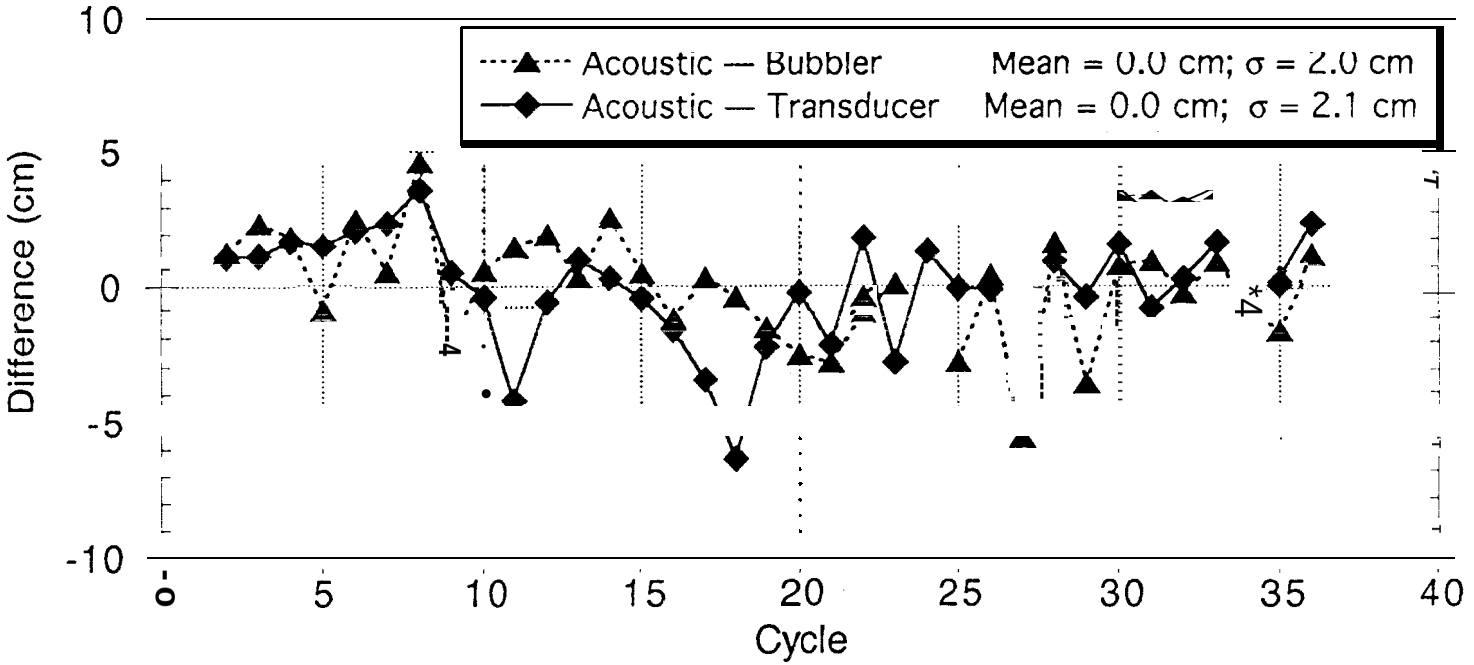

Figure 8.1

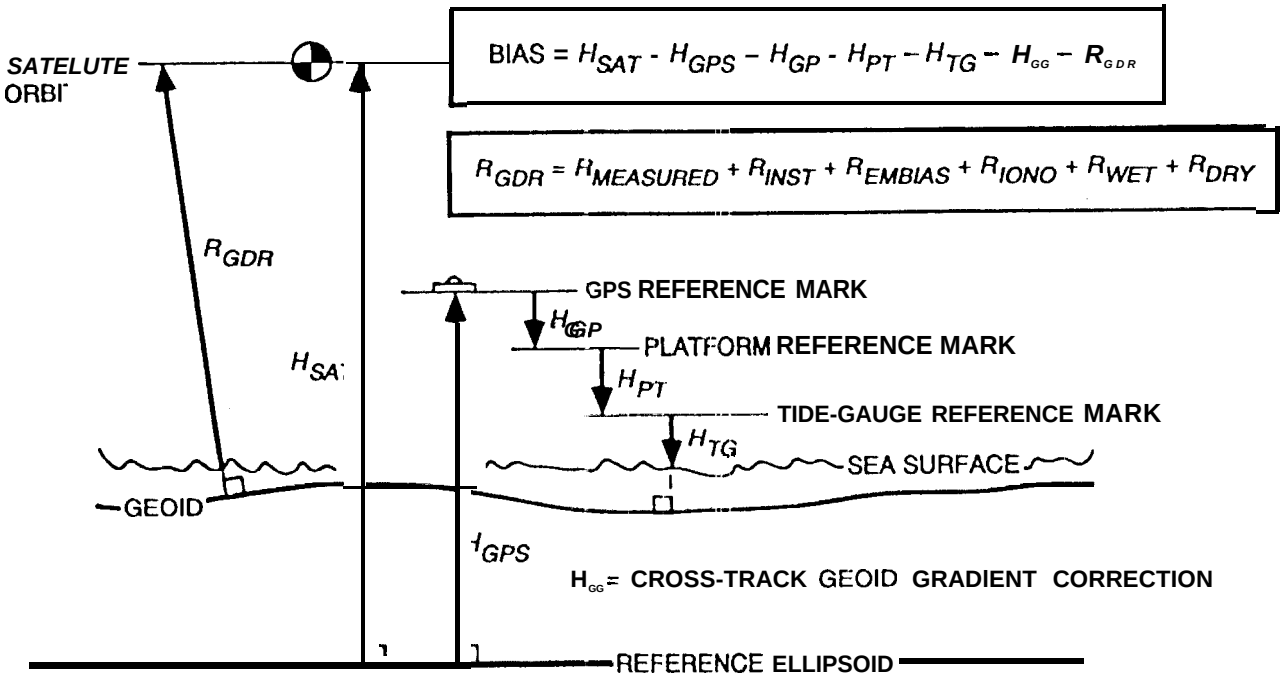

Sea-level constituents as measured by the altimeter and in situ systems.

Figure 9.1

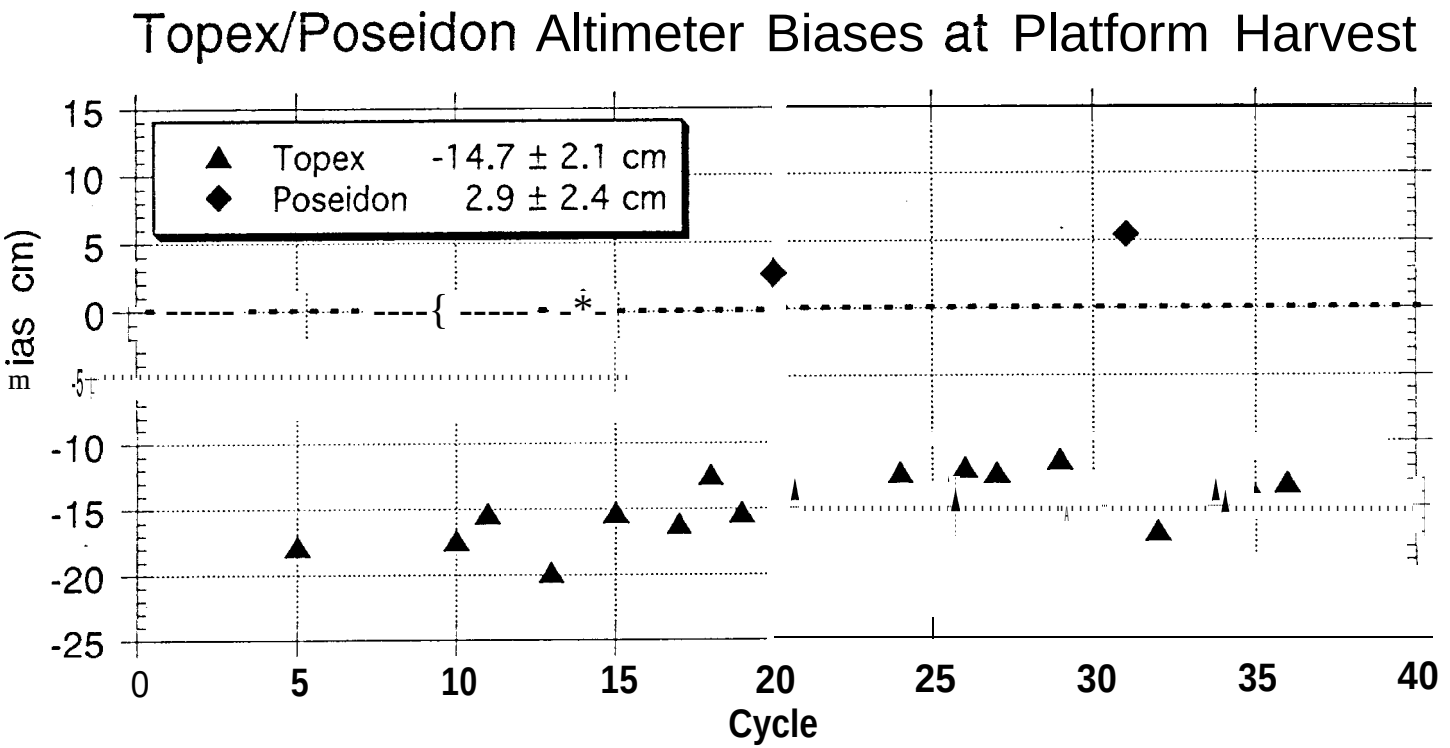
Topex/Poseidon Altimeter Biases at Platform Harvest
Topex -14.7 ± 2.1 cm
Poseidon 2.9 ± 2.4 cm
m ias cm)
15
10
5
0
-10
-15
-20
-25
0
5
10
15
20
25
30
35
40
Cycle

Figure 9.2

Table 2.1

NASA Verification Site Instrumentation

Instrument	Parameter	Responsible
Sea Level Instrumentation	Sea Level	
NGWLMS* - Acoustic		NOAA/NOS
NGWLMS* - N_2 Bubbler		NOAA/NOS
Pressure Transducers		univ. of Colorado
Rogue Global Positioning System (GPS) Receiver	Position and Columnar Total Electron Content	JPL (Sec. 335)
Water Vapor Radiometer	Columnar Water Vapor	JPL (Sec. 383)
Barometer	Atmospheric Pressure	NOAA/NOS
Hygrometer	Relative Humidity	NOAA/NOS
Thermometer	Atmospheric Temperature	NOAA/NOS
Ancillary Ocean Instrumentation	Water Temperature	NOAA/NOS
	Water Conductivity	NOAA/NOS

* NGWLMS = Next Generation Water Level Measurement System

Table 3.1

Pre-Launch Verification Site Error Budget

Source	Fixed	Variable
	(Centimeters)	
GPS Survey		
Survey Error	2.0	0.0
Platform Sway	0.0	**0.5**
Thermal Expansion of Platform (below water line)	0.0	**0.5**
Other Vertical Changes	**0.0***	**0.0**
Platform **Survey**		
Survey Error	0.5	**0.0**
Thermal Expansion of Platform (above water line)	0.0	1.0
Sea Level Measurement		
Instrument Zero	0.0	0.0
Instrument Noise	0.0	1.0
Geoid Crosstrack Variability	0.0	0.5
Ocean Spatial Variability	0.0	2.0
RSS Total	2.06	2.60
RSS Total (Fixed+Variable):	**3.32**	

* At the time of the GPS **survey.** May change **(increase)** between surveys.

Table 3.2

Laser Tracking and Altimetry Errors
For a Single Overflight

Source	RSS Error (Centimeters) Fixed	Variable
Instrument	-	**2.0**
Dry Tropospheric Correction	0.0	0.7
Wet Tropospheric Correction	0.5	0.5
Ionosphere Correction	1.0	0.5
EM-Bias	1.4	1.4
Skewness	0.0	1.0
Total Altimetry **Error**	**1.8***	**2.8**
Orbit Height Error from Laser Tracking	2.0	1.0
RSS Total	**2.69**	**2.97**

***** Does not include altimeter bias.

Table 3.3

Expected Error as a Function of Number of Overflights

Number of Overflights	Total RMS Error (centimeters)*	Variable Error Contribution (cm)*
1	5.2	3.9
3	4.9	3.6
5	4.6	3.1
10	4.1	2.3
20	3.8	1.7
30	3.7	1.4

*Includes contributions from the in situ measurements, laser tracking and altimetry. The method includes estimation of bias and bias drift.

Table 5.1

Constraints on SAO **Keplerian Elements (l-sigma)**

TFP	2006X10-3	s	~ 15 m down track position uncertainty
SMA	1.0	m	~ 1m radial position uncertainty
AOP	3.7IX1O-7	deg	~ 50 cm down track position uncertainty
OMEGA	4.5OX1O-7	deg	~ 50 cm position uncertainty
INC	2.95x10-7	deg	-50 cm position uncertainty
ECC	6.46x1 O-9		~ 50 cm radial position uncertainty

Table 7.1

Error budget for mapped TEC measurements derived from GPS

Error Source	Error (TECU)
Carrier phase noise" (30 sec. integration)	< 0.03
Antenna phase center offset (L1 vs. L2) in both receiver and satellite	<0.11
Pseudorange multipath noise	0.5 - 1.5
Receiver bias uncertainty (if calibrated)	0.6
Satellite bias uncertaintv	1.4- 2.8
RSS error for line-of-sight TEC observables	1.6- 3.2 TECU
Mapping TEC to zenith over HARVEST	1 – 5
Total (RSS) error for mapped zenith TEC	2 – 6 TECU